Synthesis of Inorganic Materials by Solvothermal Methods

05 December 2008

A. Trunschke, Department of Inorganic Chemistry,
Fritz Haber Institute, Max Planck Society

Further reading:

- K. Byrappa, M. Yoshimura, Handbook of Hydrothermal Technology, Noyes Publications, Norwich, NY, 2001.
- J.-P. Jolivet, Metal Oxide Chemistry and Synthesis – From Solution to Solid State, John Wiley & Sons Ltd., Chichester, 2000.

Outline

- Introduction
- Experimental
- Parameters governing the solvothermal reaction
- Oxide synthesis in aqueous media

Introduction

Synthesis of nanostructured catalysts and catalyst supports

Method	*advantage*	*disadvantage*
Precipitation and coprecipitation	Defect-rich materials experimentally easy	Homogeneity difficult to achieve
Sol-gel-techniques	Homogeneity of the product	Carbon-containing impurities from metal precursors
Microemulsions	Particle size control	High consumption of solvents
Solvothermal synthesis	Kinetic control over the phases formed	Predictions difficult
Solid state reactions	100% yield stoechiometric reaction Highly crystalline products	Most thermodynamically stable phases are obtained Low surface area, particle size is difficult to control
Flame pyrolysis	Particle size control	
Chemical vapor deposition		
Molten salt synthesis		

Solvothermal methods in inorganic synthesis

Solvothermal reaction:
Any heterogeneous chemical reaction in a closed system, in the presence of a solvent and temperature above the boiling temperature of the solvent used

Autoclave/Parr

- Autogeneous pressure: self developed pressure, not externally applied
- Mineralizer: component that helps to dissolve the reactants by forming complexes, which are more soluble
  (e.g. alkali metal hyroxide in silicate synthesis)

Under solvothermal conditions, reactants which are otherwise difficult to dissolve go into solution under the action of mineralizers or solvents

Historical development

1845-1900 Mineral synthesis, imitation of natural conditions

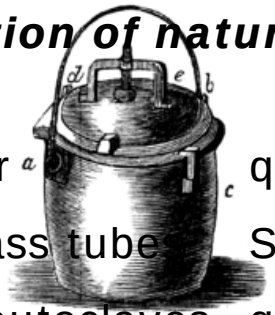

1845	K.E. von Schafhäutl	Papin's digestor	quartz crystals
1848	R. Bunsen	thick walled glass tube	Sr, Ba carbonates
1851	H. de Sérnamont	glass tubes in autoclaves (steel tubes) founder of hydrothermal synthesis in geoscience	quartz, carbonates, sulfates, sulfides, fluorides
1873	K. von Chrustschoff	Au lining	prevent corrosion
1890	C. Doetler	Ag-lined steel tube closed by a screw cap and Cu washer	mineral recrystallization
1892	C.J. Bayer	invention of the first indutrial hydrothermal process (hydrometallurgy)	leaching of Bauxite with NaOH at 170-180°C

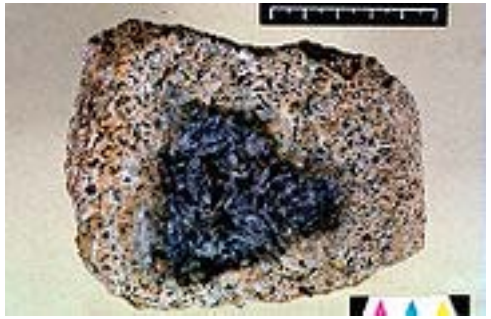

$$Na[Al(OH)_4] \rightleftharpoons Al(OH)_3 + NaOH$$
$$Na[Fe(OH)_4] \rightleftharpoons Fe(OH)_3 + NaOH$$

Historical development

1900-1950 Mineral synthesis, improvements in pT conditions

1914 G.W. Morey — standard „Morey-type“ autoclave

J. Am. Chem. Soc.; 1914; 36(2) pp 215 - 230; New Crystalline Silicates of Potassium and Sodium, their Preparation and General Properties.

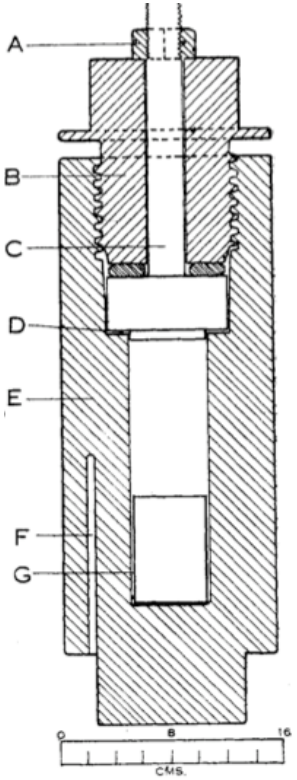

Fig. 1.—Diagram showing the construction of the bomb used.

1943 R. Nacken — fundamentals of industrial growth of quartz crystals using seeds

1948 R.M. Barrer — synthesis of zeolites

J. Chem. Soc., 1948, 2158 - 2163; Syntheses and Reactions of Mordenite

1949 O.F. Tuttle — cold seal and test tube autoclaves

1900-1950 **Mineral synthesis, improvements in pT conditions**

435. *Syntheses and Reactions of Mordenite.*

By R. M. Barrer.

Mordenite has been crystallised in good yield from aqueous suspensions of sodium aluminosilicate gels of compositions ranging from $Na_2O,Al_2O_3,8{\cdot}1SiO_2,nH_2O$ to

$$Na_2O,Al_2O_3,12{\cdot}3SiO_2,nH_2O,$$

the best temperature range being 265—295°; pH is as important as composition or temperature in ensuring a yield, and the best results were for a range of pH between 8 and 10 in the cold mother-liquor after crystallisation.

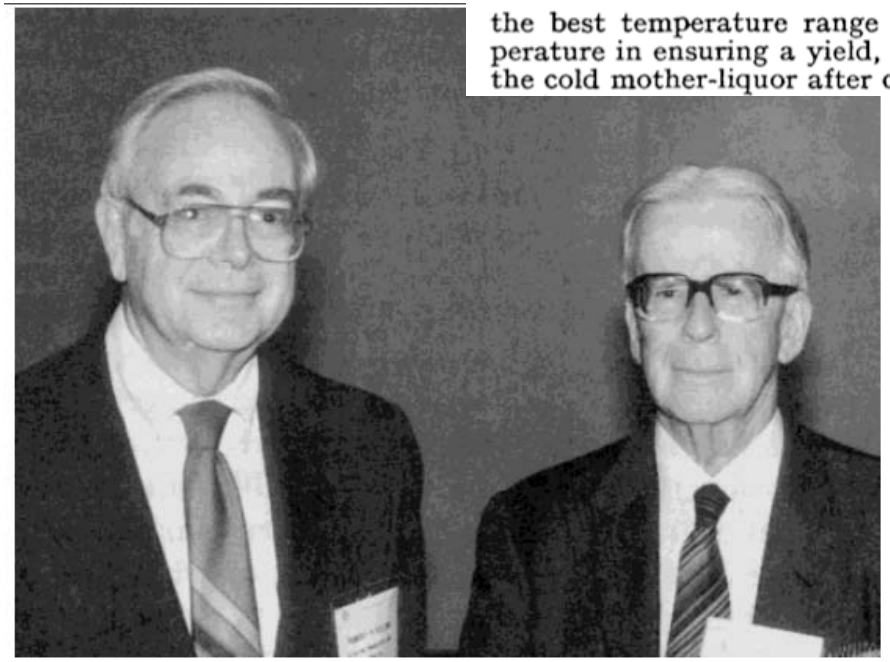

Figure 2. The Founding Fathers. R. M. Barrer (1910–1996) (right) and R. M. Milton (1920–2000) photographed by M. L. Occelli at the ACS Symposium in Los Angeles on September 22, 1988. (Reprinted with permission from ref 33. Copyright 1989 American Chemical Society.)

Work by Milton at the labs of Linde corporation:

Synthesis of zeolite A, zeolite X

Historical development

mazzite = ZSM-4
tschernichite = zeolite beta
mutinaite = ZSM-5

1950-today

1950-1960	phase diagrams for natural systems
1960-1980	synthesis of technologigal materials new inorganic compounds without natural analogs or synthesis before discovery
1980-1990	importance of the technique in materials science physical chemistry of hydrothermal solutions
> 1990	diversification of hydrothermal techniques solvothermal synthesis entry of organic chemists physical chemistry of hydrothermal solutions design of new reactors: batch reactors, flow reactors

Novel applications of solvothermal synthesis

Field	Application
Synthesis of different material families	□Oxides, halogenides, chalcogenides □Nitrides, carbides, phosphides □Metallics, intermetallics □Open-framework and hybrid materials
Synthesis of new phases or stabilization of new inorganic compounds with specific structures and properties	□Functionalized materials □Nanostructures (rods, wires, tubes) □Magnetic nanoparticles □Preparation of materials with narrow particle size distribution and homogeneous microstructure (morphology control of transition metal oxides)
Crystal growth and modification	□Synthesis of single crystals of low temperature forms with low density of defects □Decomposition, dissolution, corrosion, etching
New process developments	□Large-scale synthesis □Synthesis of nanoparticles with supercritical fluids □Morphology control with microwave-hydrothermal synthesis

Synthesis of microporous alumosilicates

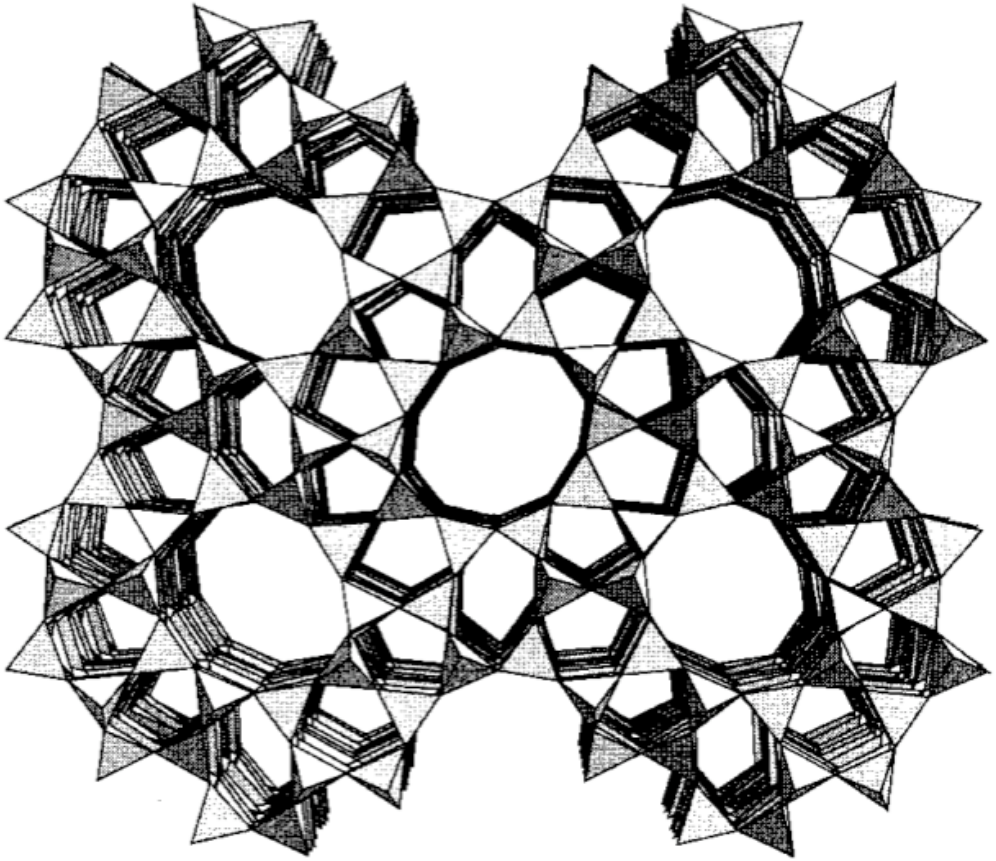

Zeolite ZSM-5 (MFI)

Classical applications of synthetic zeolites

- Ion exchangers
- Molecular sieves
- catalysts

A. K. Cheetham, G. Ferey et al. Angew. Chem. Int. Ed. 38 (1999) 3268-3292.

Open framework structures of transition metal phosphates

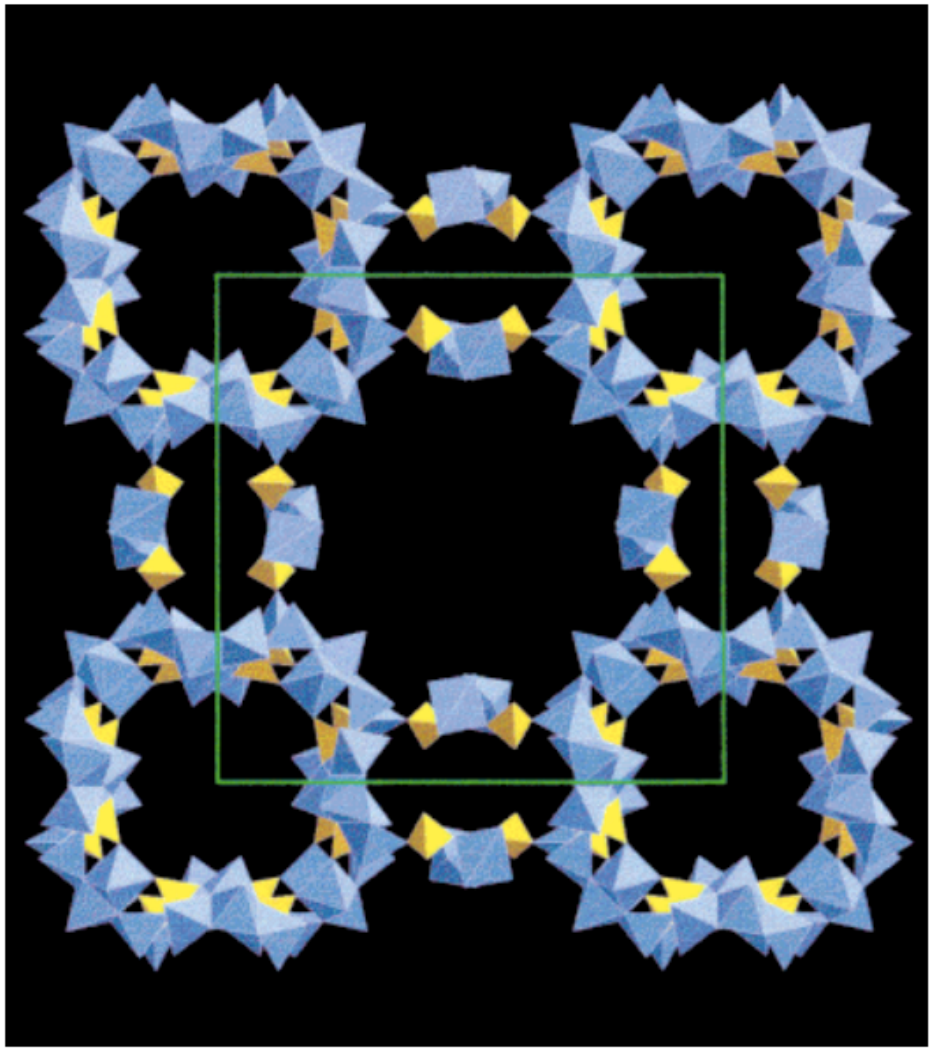

Figure 15. A view of the open framework of $Cs_3[V_5O_9(PO_4)_2] \cdot x\,H_2O$. The Cs and H_2O are not shown.

M. I. Kahn, L. M. Meyer, R. C. Haushalter, A. L. Schweitzer, J. Zubieta, J. L. Dye, Chem. Mater. 8 (1996) 43.

Experimental

Autoclaves: batch experiments

250°C
60 (200) bar

Autoclave/Premex AG

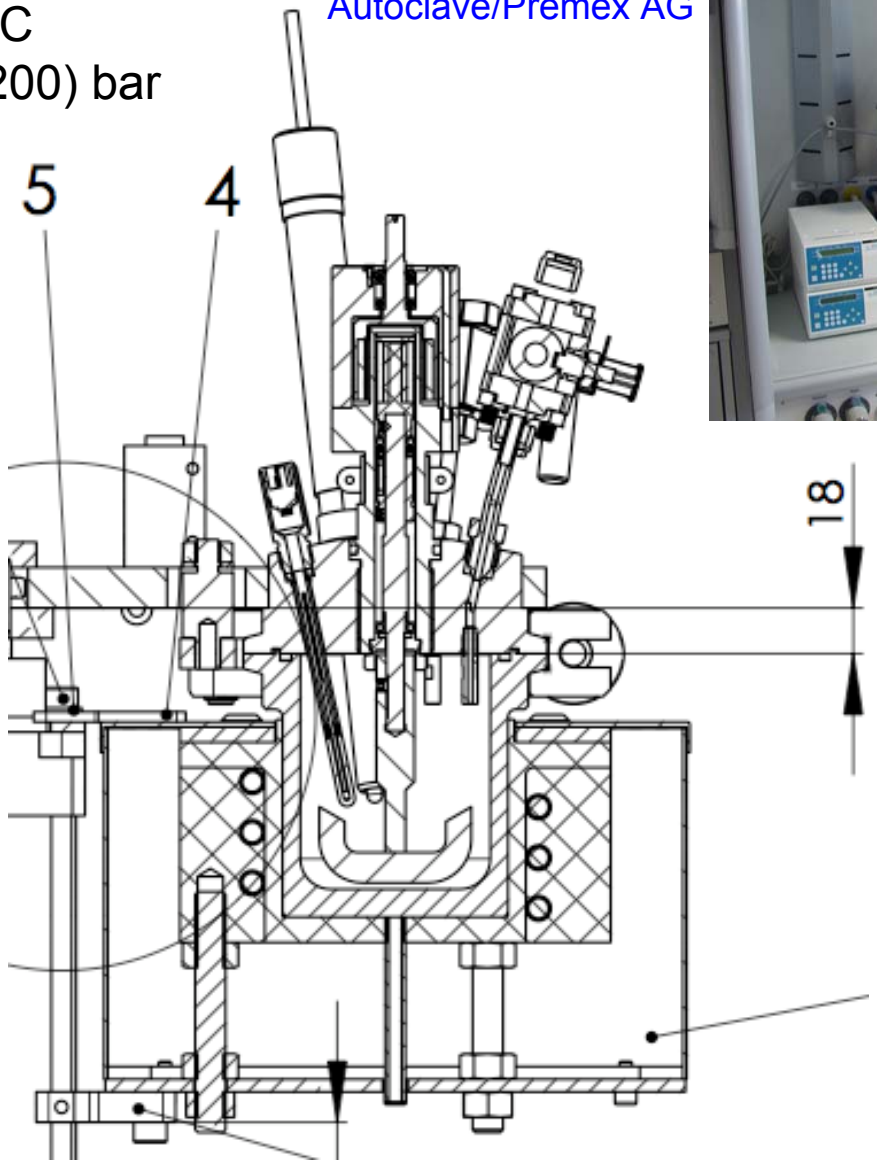

control unit

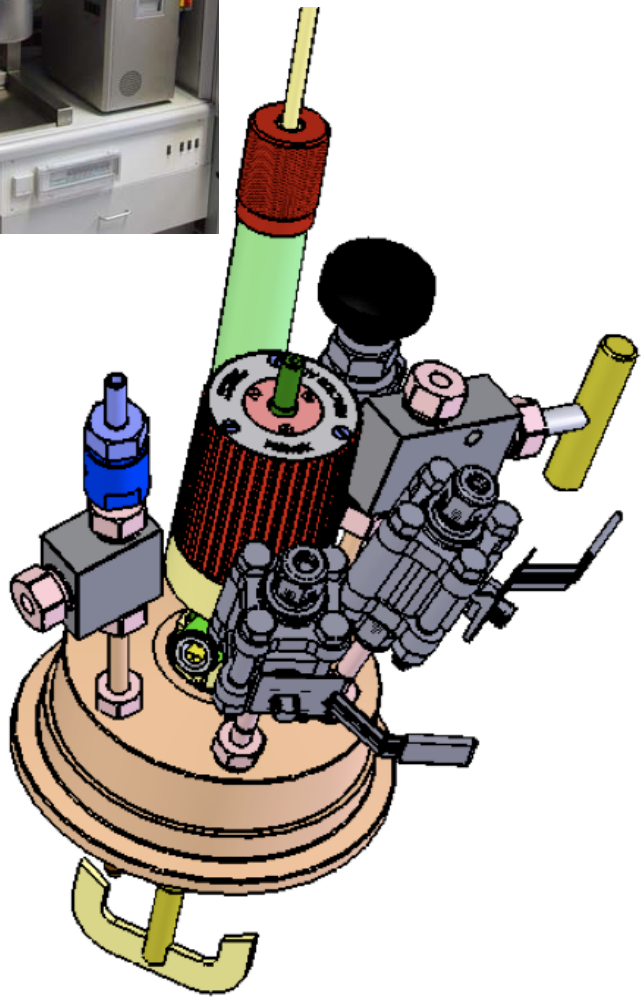

Autoclaves: flow experiments

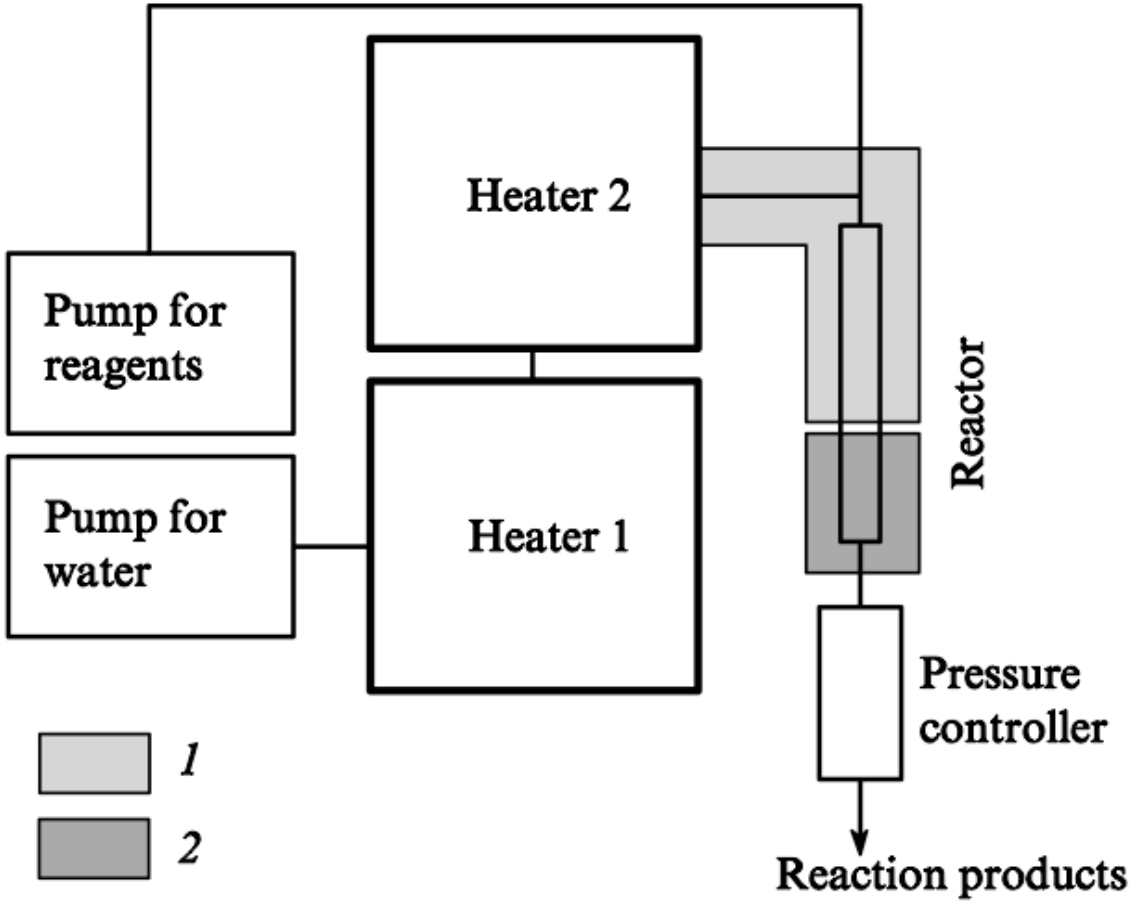

Figure 6. Scheme of an experimental flow reactor for operation with subcritical and supercritical water.
Heating zone (*1*) and cooling zone (*2*).

A. A. Galkin, V. V. Lunin, Russian Chemical Reviews 74 (1) (2005) 21-35.

Material properties

Table 3.2. Properties of Certain Alloys.[2] *(Courtesy of the Academic Press, Orlando, Florida.)*

	Resistance to aqueous OH	Rupture stress (atm) 1000 h, 800°C	Rupture stress (atm) 1000 h, 600°C
Low carbon steel	+		170
Tool steel	+		
4140 (similar to EN19)	+		170
Stainless type 340	—	270	1100
19-9-DL	?	680	2200
(Universal Cyclops Steel Co.)			
Croloy 15-15N	+	610	2260
Timken 17-22-A	+	-	-
Inconel X	?	1200	4500
Stellite	?	-	-
Udimet 500	?	2100	-
Silver	+ [b]		
Platinum	+ [b]		
Platinum-10% irridium	+ [b]		

Source: Data from Clauss (1969)
[a] Cr and Ni values in stainless steels are values < 2 wt %.
[b] Denotes the balance of metal in the alloy.
[c] A product of Allegheny Ludlum Steel Corporation, Pittsburgh, Pennsylvania.
[d] A product of Inco Alloys International, Inc., Huntington, West Virginia.
[e] A product of Cabot Corporation, Kokomo, Indiana.

Table 3.3. Compositions of High-Strength Alloys for Autoclaves

	Metal Content (wt %)												
	Cr	Ni	C	Mn	Mo	Si	Co	V	Al	Ti	Fe	Others	Note
Stainless Steel [a]													
304	19	9	0.1	2	-	1	-	-	-	-	ba[b]		
310	25	20	0.2	2	-	1	-	-	-	-	ba		
316	17	12	0.1	2	3	1	-	-	-	-	ba		
410	12	-	0.2	1	-	1	-	-	-	-	ba		
Titanium													
RMI-55	Commercially pure titanium												Alpha
Ti6-4	—	—	0.1	—	—	—	—	4	6	ba	0.25		Alpha-beta phase
Ti38644	6	—	0.05	—	4	—	—	8	3	ba	0.03	Zr-4	Beta phase
Ti17	4	—	—	—	4	—	—	—	5	ba	—	Zr-2, Sn-2	Alpha-beta
Superalloys													
A-286	15	25	0.1	2	1	1	—	0.2	0.4	2	ba		Iron base
Waspalloy[c]	19	ba	0.1	1	4	0.7	13	—	1	3	2	Cu-0.5	Nickel base
Inconel 702[d]	16	ba	0.1	1	—	0.7	—	—	3	0.5	2	Cu-0.5	Nickel base
Hastelloy B[e]	1.0	ba	0.05	1	28	1	2.5	0.4	—	—	5	—	Nickel base
Hastelloy C[e]	16	ba	0.1	1	16	1	2.5	0.4	—	—	5	W – 4	Nickel base
HS – 21	27	3	0.3	1	5	1	ba	—	—	—	2		Co base (stellite)

Source: Data from Clauss (1969)
[a] Cr and Ni values in stainless steels are values < 2 wt %.
[b] Denotes the balance of metal in the alloy.
[c] A product of Allegheny Ludlum Steel Corporation, Pittsburgh, Pennsylvania.
[d] A product of Inco Alloys International, Inc., Huntington, West Virginia.
[e] A product of Cabot Corporation, Kokomo, Indiana.

Material properties

Table 3.4. High-Temperature Strength Properties of Autoclave Alloys[a]

Melt	Tensile Strength (°C)			Yield Strength (°C)			Creep Rupture Strength (hr)		Creep Strength (hr)		Thermal Expansion ($\times 10^6$)
	25	400	600	25	400	600	1,000	10,000	1,000	10,000	
Stainless Steels											
304	85	66	49	38	21	16	49	38	24	18	14
310	92	81	71	40	29	24	39	36	23	14	16
316	85	72	66	38	24	21	66	64	31	19	16
410	89	72	34	32	22	13	34	26	29	14	11
Carbon Steel											
0.3% C	64	57	25	36	25	16	19	12	—	10	12
Superalloys											
A-286	143	-	103	94	-	88	88	76	—	81	—
Waspalloy	180	-	170	115	-	100	85[b]	—	—	—	—
Inconel	141	-	105	85	-	75	65[c]	—	—	—	—
Hastelloy C	121	-	98	58	-	43	55[d]	—	—	—	—
HS-21	101	-	73	82	-	39	60[e]	—	—	—	—
Titanium Alloys											
RMI-55	65	30	20	55	18	10	20[f]	—	—	—	8
Ti 6-4	130	90	60	120	70	55	50	30	30	20	8
Ti 38644	170	150	120	160	130	90	140[g]	—	100	—	5
Ti 17[h]	—	—	—	(150–170)			—	—	—	—	—

Source: Data from Clauss (1969)

[a] Strength in 100 pounds per square inch (kpsi), yield strength is for 0.2 elongation, creep strength is for 1% elongation unless otherwise noted.

[b-c] For 1000 hr at 650°C.

[f] For 100 hr at 450°C.

[g] For 100 hr at 350°C and 0.2% elongation.

[h] Data from RMI Company, Niles, Ohio.

Table 3.5. Materials Used as Reactor Linings

Material	T (°C)	Solutions	Remarks
Titanium	550	chlorides hydroxides sulphates sulphides	Corrosion in NaOH solution > 25% in NH_4Cl solution > 10% (at 400°C)
Armco iron	450	hydroxides	Gradual oxidation producing magnetite
Silver	600	hydroxides	Gradual recrystallization and embrittlement, partial dissolution
Platinum	700	hydroxides chlorides sulphates	Blackening in chlorides in the presence of sulpher ions; partial dissolution in hydroxides
Teflon	300	chlorides hydroxides	Poor thermal conduction
Tantalum	500	chlorides	Begin to corrode in NH_4Cl solution 78%
Pyrex	300	chlorides	
Copper	450	hydroxides	Corrosion reduced in the presence of fluoride ions and organic compounds
Graphite	450	sulphates	Pyrolytic graphite most suitable for linings
Nickel	300	hydroxides	
Quartz	300	chlorides	
Gold	700	hydroxides sulphates	Partial dissolution in hydroxides

Water in a closed vessel

Pressure inside a sealed vessel as a function of percentage fill and temperature

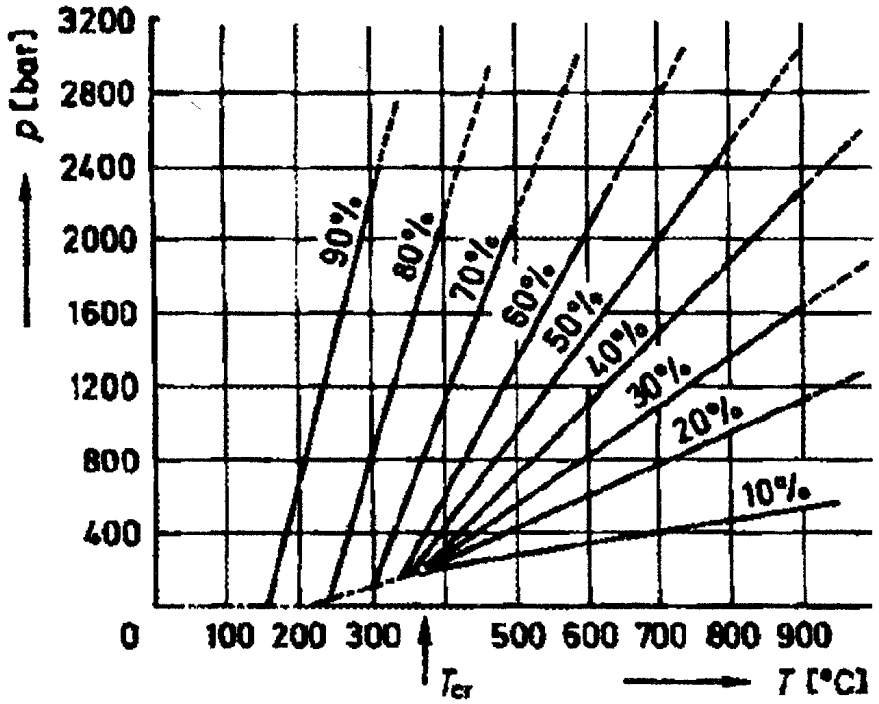

critical fill 32%

ρ_{cr} = 0.32 g/cm^3

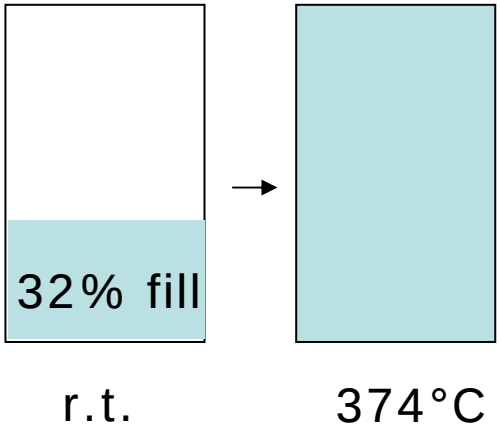

A. Rabenau, Angew. Chem. 97 (1985) 1017-1032.

Other solvents

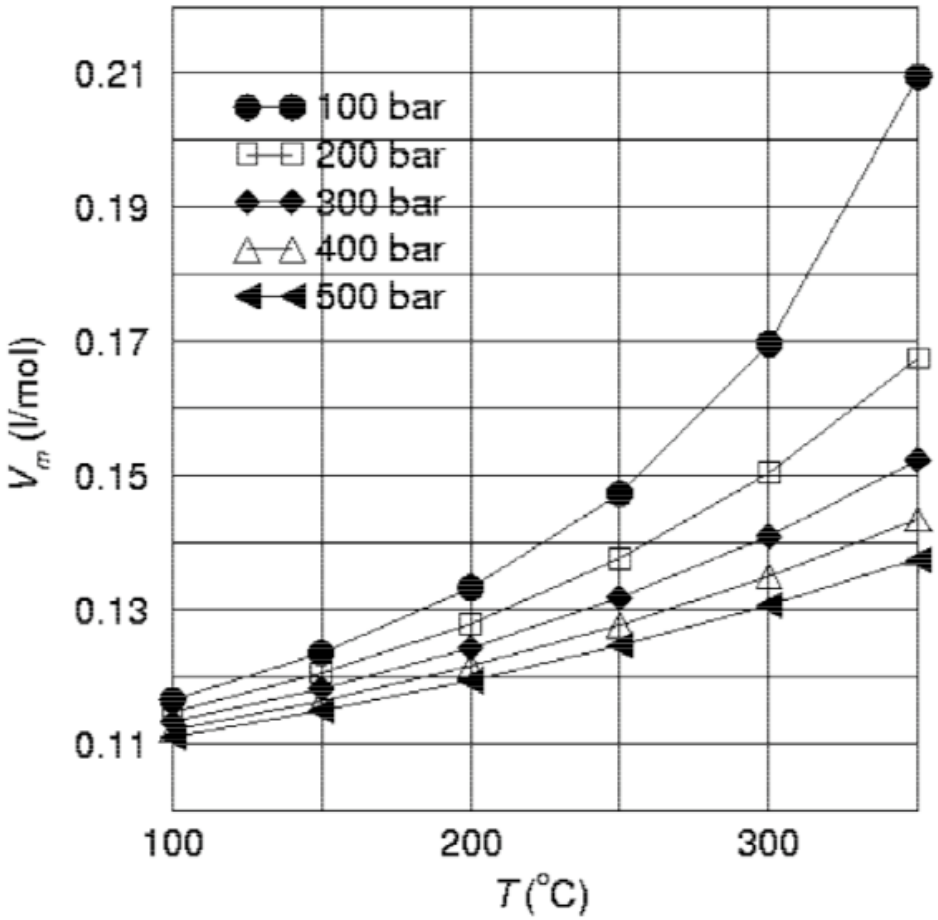

Fig. 1. Isobars displaying the dependence of the starting molar volume of toluene taken in a closed bomb, on the temperature. The isobars were obtained using the Peng–Robinson equation of state as explained in the text.

$$p = [RT/(V_m - b)] - [a/(V_m^2 + 2bV_m - b^2)]$$

The parameters a and b are given by:

$$a = 0.45724 R^2 T_C^2 [1 + f_\omega (1 - T_r^{1/2})]^2 / p_C$$

$$b = 0.07780 R T_C / P_C$$

$$f_\omega = 0.37464 + 1.54226\omega - 0.26992\omega^2$$

ω *acentric factor (tabulated)*

$$\omega = -\log\left(\frac{P_s}{P_c}\right)_{T_r=0,7} - 1$$

$T_r = T/T_C$

M. Rajamathi, R. Seshadri, Current Opinion in Solid State and Materials Science 6 (2002) 337-345.

Savety

100 cm^3
20 000 psi

≈

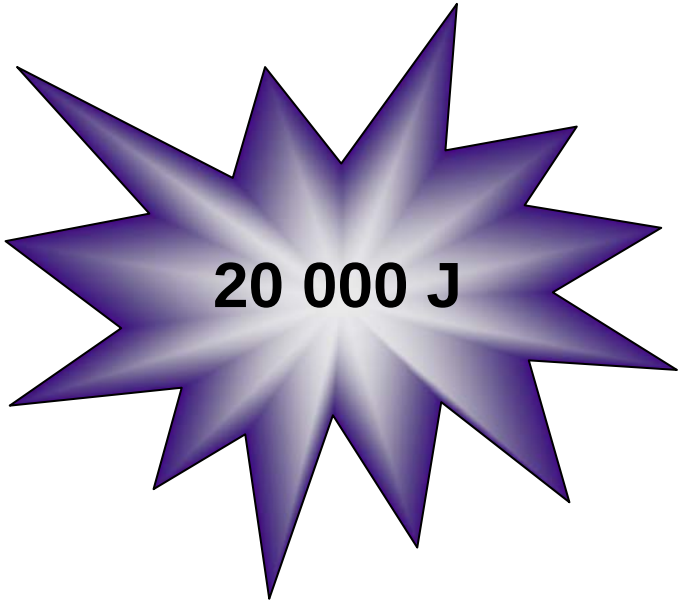

Important:

- Maintenance of the autoclave
- Anticipation of the dangers of hydrothermal experiments

Savety

- Consider the technical parameters of the autoclave
- Use rupture discs calibrated to burst above a given pressure
- Make provision to vent the live volatiles out in event of rupture
- Use proper shielding (close the fume hood)
- New autoclaves should be heated with distilled water in the vessel several times
- Once a vessel has contained reduced sulfur, it should not be used for sulfur-free experiments unless it has been vacuum cleaned while hot, followed by heating in air at 350°C
- Do not quench the vessel rapidly
- Undertake precaution to prevent overheating of the furnace resulting from malfunction of the control system
- Hot surfaces! Wear special insulated gloves 
- The vessel to be heated must never be filled completely with aqueous solution
- Calculate the thermal expansion of the aqueous phase and allow at least 20% of total volume of the vessel for uncertainty or temperature overturn, consider the formation of gases

Parameters governing the solvothermal reaction

Types of hydrothermal reactions

Dissolution, precipitation and modification of precipitates, flocculates, gels or colloids under aging or ripening

- Redox reactions

$$2In^{3+} + 3CH_3CH_2OH \rightarrow 2In + 3CH_3CHO + 6H^+$$

$$S_2O_3^{2-} + 2H^+ \rightarrow S + SO_2 + H_2O$$

$$2In + 3S \rightarrow In_2S_3$$

- Hydrolysis

$$[M(OH_2)]^{z+} \leftrightharpoons [M{-}OH]^{(z-1)+} + H^+ \leftrightharpoons [M{=}O]^{(z-2)+} + 2H^+$$

$$Si(OR)_4 + nH_2O \rightarrow Si(OR)_{4-n}(OH)_n + nROH$$

- Thermolysis
- Complex formation
- Metathesis reactions

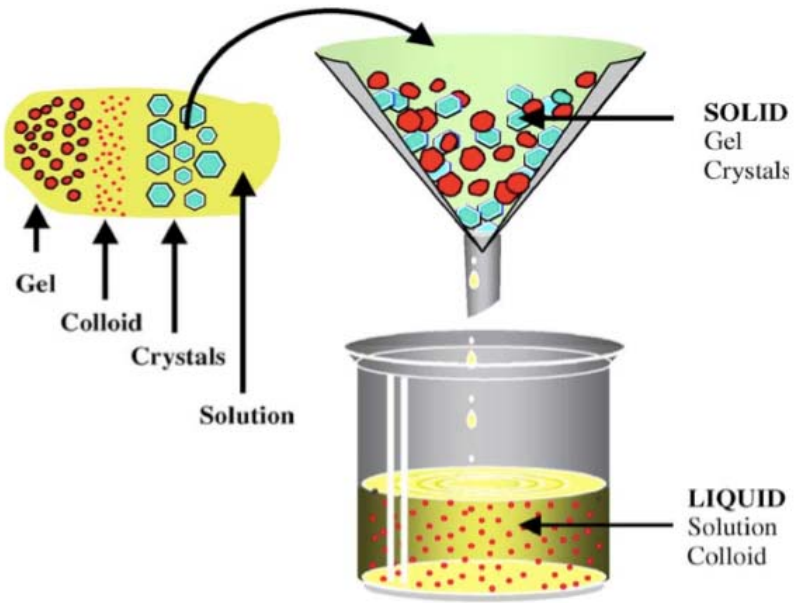

C.S. Cundy, P.A. Cox, Microporous and Mesoporous Materials 82 (2005) 1–78.

Hydrothermal transformations

For what purpose do we apply hydrothermal conditions?

Metastable, more complex structures are favoured involving smaller enthalpy and entropy changes than standard conditions

Small crystals or amorphous particles	→	Large crystals or amorphous particles
Amorphous material	→	Crystalline material
Crystal 1	→	Crystal 2

Main parameters governing the hydrothermal reaction

- Thermodynamic parameters (T, p)
- Kinetics
- Chemical parameters
  - Solvent
  - Chemical composition of the precursor
  - Concentration
  - pH, ionic strength
  - Complexing agents
  - Reducing / oxidizing agents
  - Templates
- Experimental parameters
  - Volume / wall ratio
  - Wall material
  - Heat exchange
  - Stirrer speed
  - Cooling facilities

Mechanism of oxide formation in hydrothermal synthesis

A

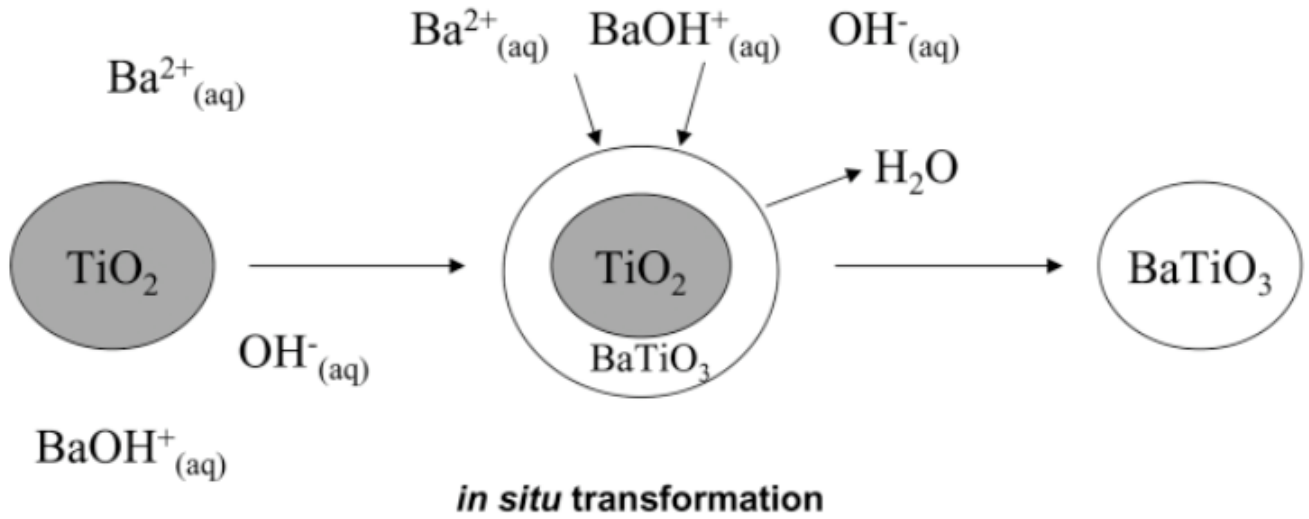

***in situ* transformation**

B

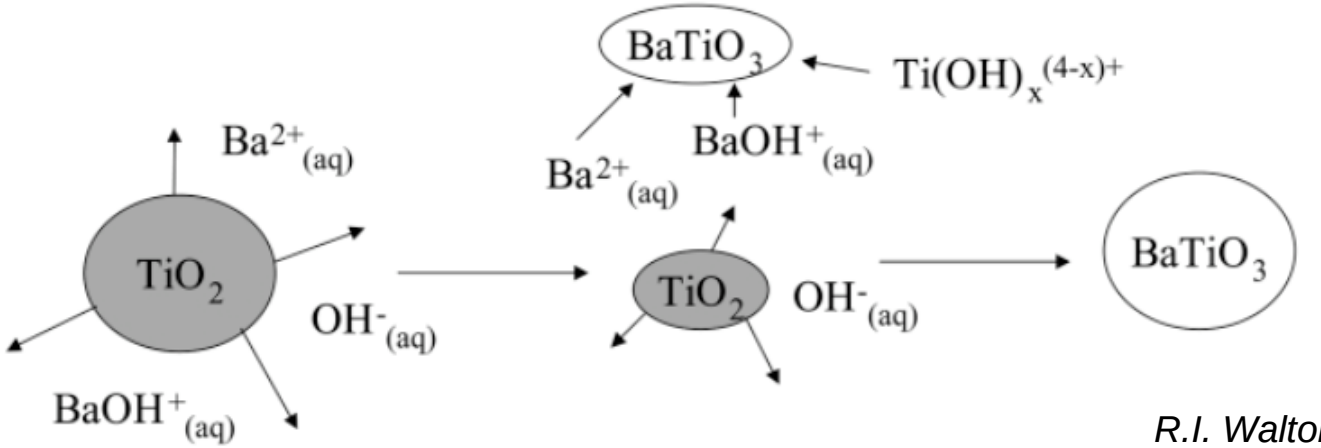

dissolution-precipitation

R.I. Walton, Chem. Soc. Rev. 31 (2002) 230–238.

Hydrothermal conditions

- Strength of acids and bases is changed
  - Condensation of metal cations is linked to the their acid-base characteristics
- Forced hydrolysis of cations (thermohydrolysis)
- Modification of the chemistry of cations in solution
  - Coordination of cations with unusual symmetry

The kinetics of solid transformation in suspensions are accelerated

The properties of the **solvent** are significantly influenced by T and p

Water as a polar protic solvent

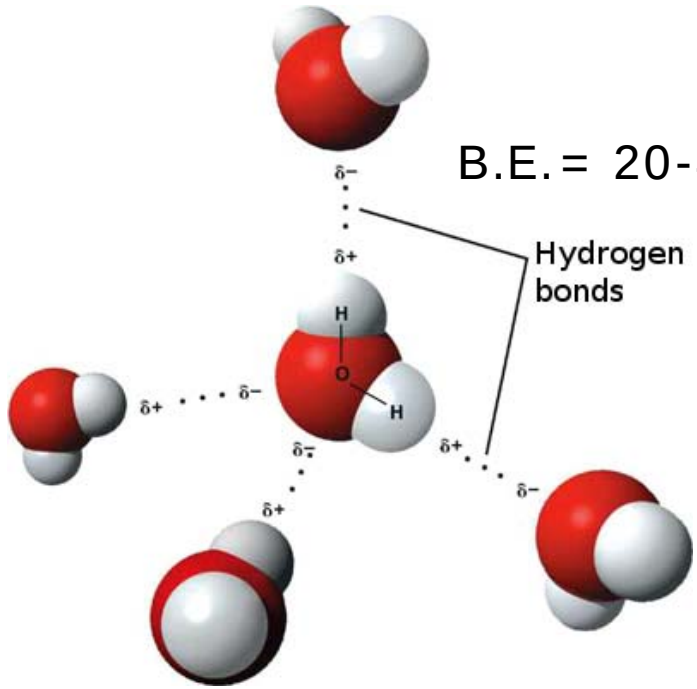

B.E. = 20-40 kJ mol^{-1}

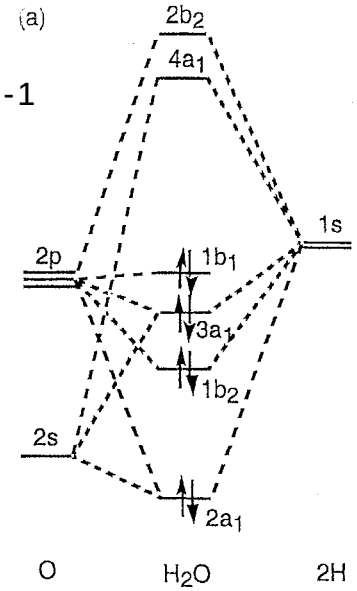

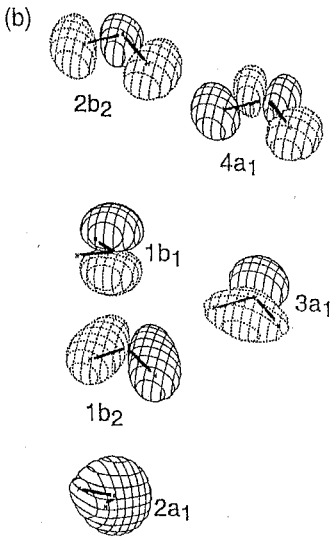

The high polarity of water is responsible for solvation of metal ions

- Solvation of cations: Water has Lewis base character due to the electrons in the $3a_1$ MO (nucleophilic interaction with Lewis acids)
- Solvation of anions: Electrophilic interaction by formation of hydrogen bonds

Schematic phase diagram of water

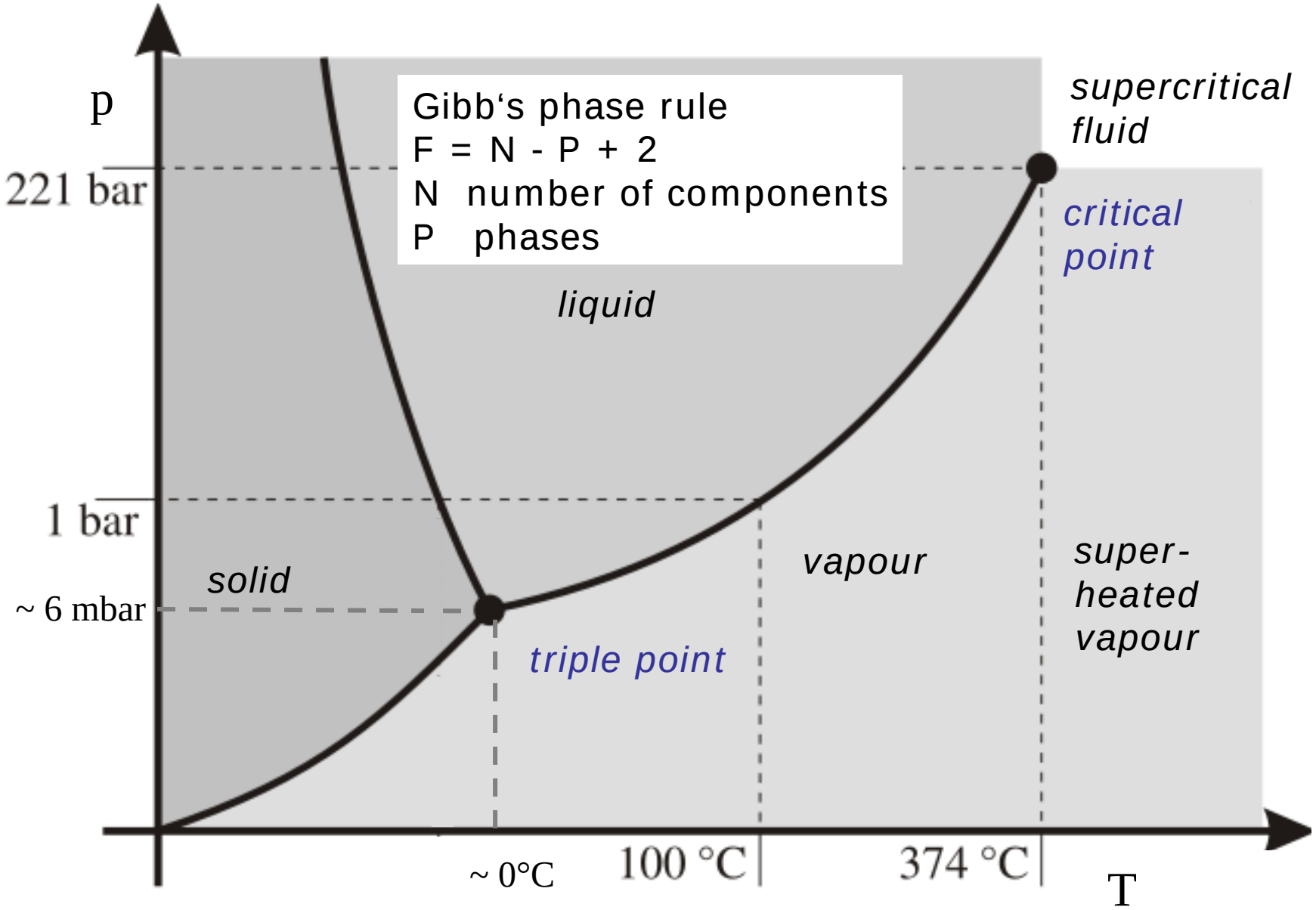

Characteristics of water under different conditions

Characteristic	Water under normal conditions	Supercritical water	Super-heated steam
T /K	298	723	723
P /MPa	0.1	27.2	1.4
ρ /kg m^{-3}	998	128	4.19
D /m^2 s^{-1} (see [a])	7.74×10^{-8}	7.67×10^{-6}	1.79×10^{-5}
Thiele modulus	2.82	0.0284	0.0122
ε	78	1.8	1.0
$-\log K_w$	14	21	41
Solubility of O_2/C_xH_y /kg m^{-3}	8×10^{-3}/?	∞/∞	∞/?

[a] Diffusion coefficient.

- The characteristics of supercritical water are intermediate between those of liquid and gas
- Physico-chemical properties change continuously

Density

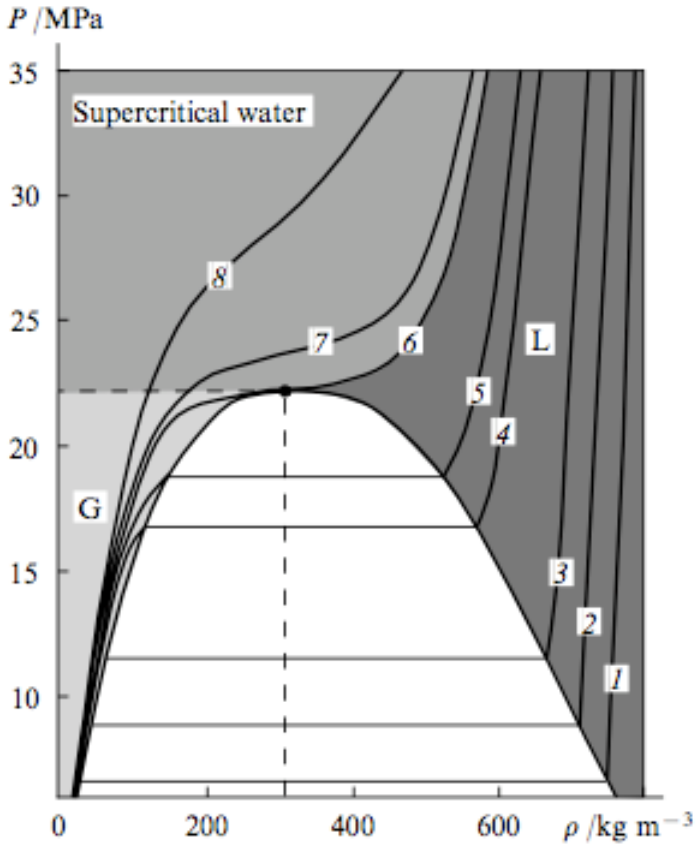

Figure 1. Phase diagram of water at elevated temperatures and pressures. T / K: 553 (*1*), 573 (*2*), 593 (*3*), 623 (*4*), 633 (*5*), 647 (*6*), 653 (*7*) and 673 (*8*); G is gas and L is liquid.

Infinite compressibility of water in the near critical region -

Density variations over a wide range by only slightly varying
T and p

Viscosity

$$(H_2O)_i + (H_2O)_1 \overset{K_i(T)}{\rightleftarrows} (H_2O)_{i+1} \qquad i = 1,2,\ldots,\infty.$$

K_i decreases as T increases ($\Delta_R H<0$)

298 K: up to 100 molecules in one cluster

673 K: 50% of hydrogen bonds broken

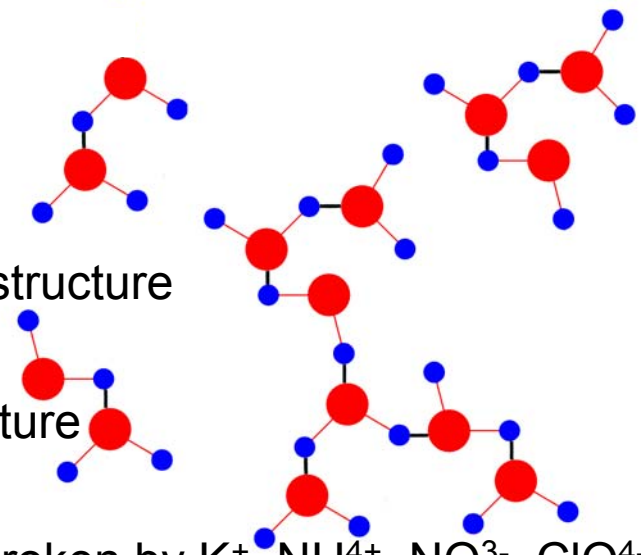

Under supercritical conditions the clusters have chain structure

- Viscosity of water decreases with increasing temperature
- Mobility of dissolved species increases
- Viscosity changes in presence of ions: H-bonds are broken by K^+, NH^{4+}, NO^{3-}, ClO^{4-}
- Weakly polarizing ions ($[NR_4]^+$, R=CH_3, C_2H_5,…) are incorporated within the solvent - formation of polyhedral cages

Dielectric constant

macroscopic property $\varepsilon_r = \frac{C_x}{C_0}.$

ε<15 ***nonpolar solvent***

ε>15 ***polar solvent***

- The dielectric constant of water decreases with increasing temperature and increases as pressure increases
- The solvation is affected: Under supercritical conditions water molecules cannot sufficiently screen ions - electrolytes form ion pairs

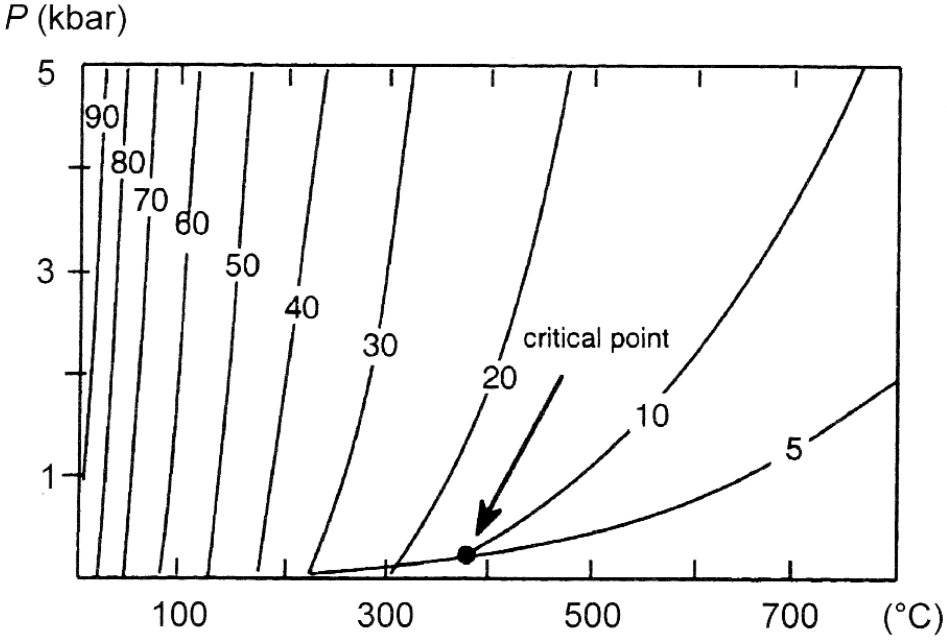

Ionic product

$$2\,H_2O \rightleftharpoons H_3O^+_{solv.} + OH^-_{solv.}$$

$K_e = a_{H^+} \cdot a_{OH^-}$	$= 1.00 \cdot 10^{-14}$	at T=298 K	pH=7
	$= 74 \cdot 10^{-14}$	at T=373 K	pH=6.07

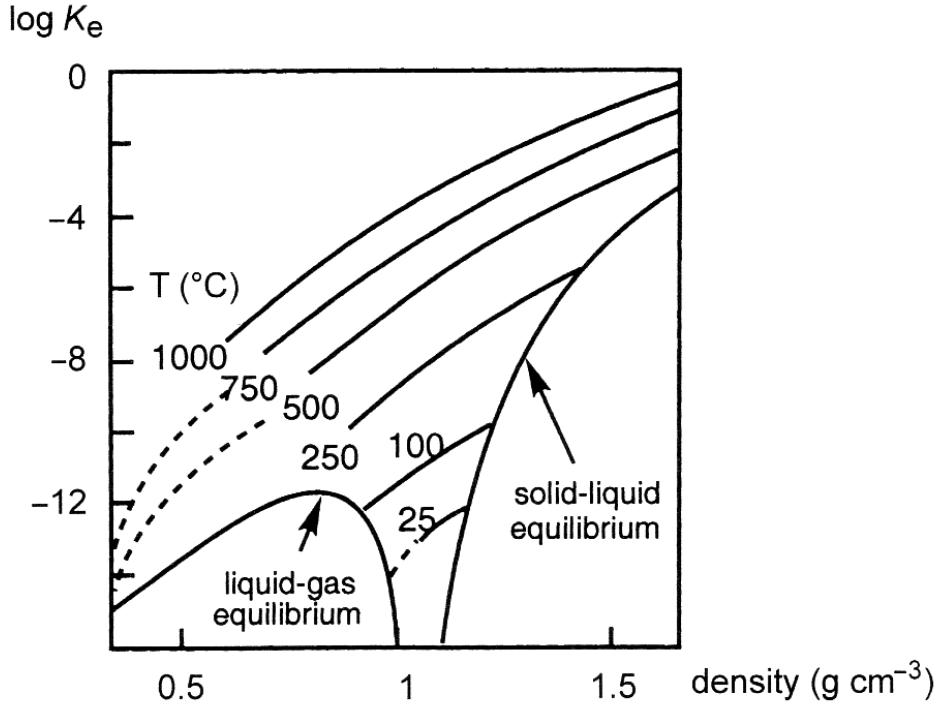

- The ionic product of water strongly increases with temperature
- sub-critical water is a rich source of H^+ and OH^-
- supercritical water shows properties of an ionic liquid at very high p and T

Redox potential

$$MnO_4^- + 8\,H^+ + 5\,e^- \rightleftharpoons Mn^{2+} + 4\,H_2O$$

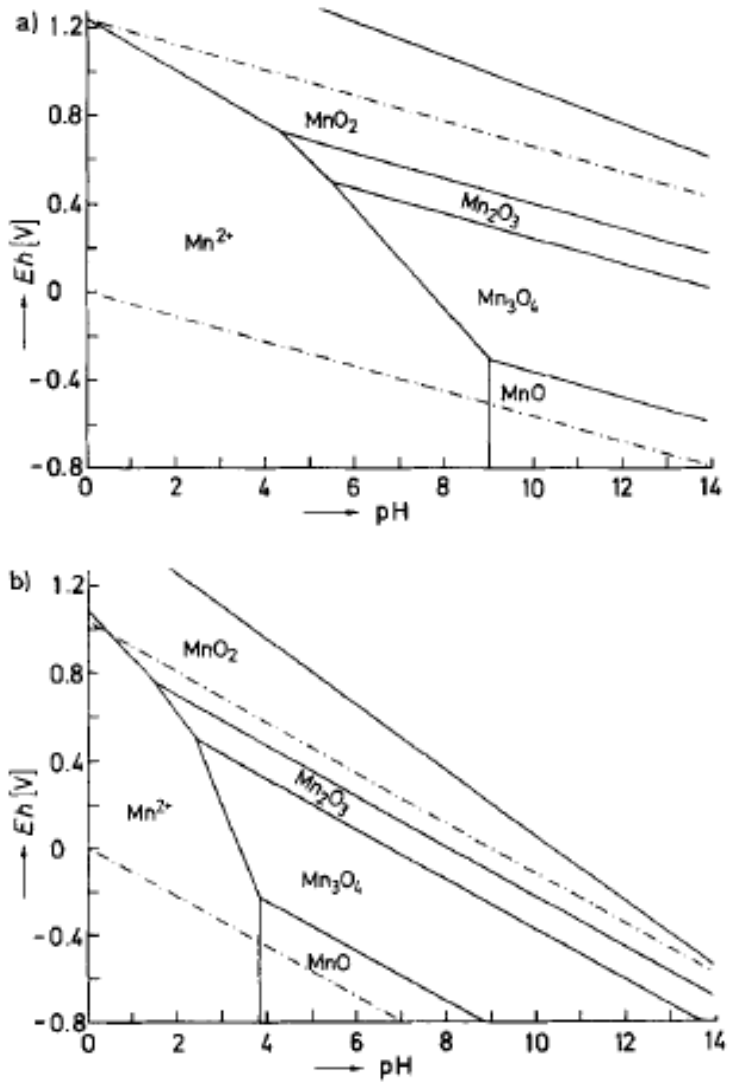

Fig. 15. *Eh*-pH diagram of the Mn-H_2O system at a) 25°C; b) 300°C [129].

A. Rabenau, Angew. Chem. 97 (1985) 1017-1032.

Other parameters

- In ***concentrated solutions*** the critical temperature is higher – below 800°C no differentiation between sub- and supercritical conditions possible
- ***Additives to control the oxidation state***
  - Hydrolysis of metal acetates, formates, and oxalates involves CO formation, CO is more soluble in water under hydrothermal conditions
  - Hydrocarbon ligands favour the formation of reduced nanoparticles
  - Oxidazing agents: H_2O_2, $HClO_4$, HNO_3, Cl_2, Br_2, O_2
- Formation of ***specific structures or morphology*** by addition of complexing agents, structure directing agents and templates

Tetramethylammonium cations occluded into the sodalite cage

G.J. de A.A. Soler-Illia, C. Sanchez, B. Lebeau, J. Patarin, Chem. Rev. 102 (2002) 4093.

Oxide synthesis in aqueous media

Mechanism of oxide formation in hydrothermal synthesis

A

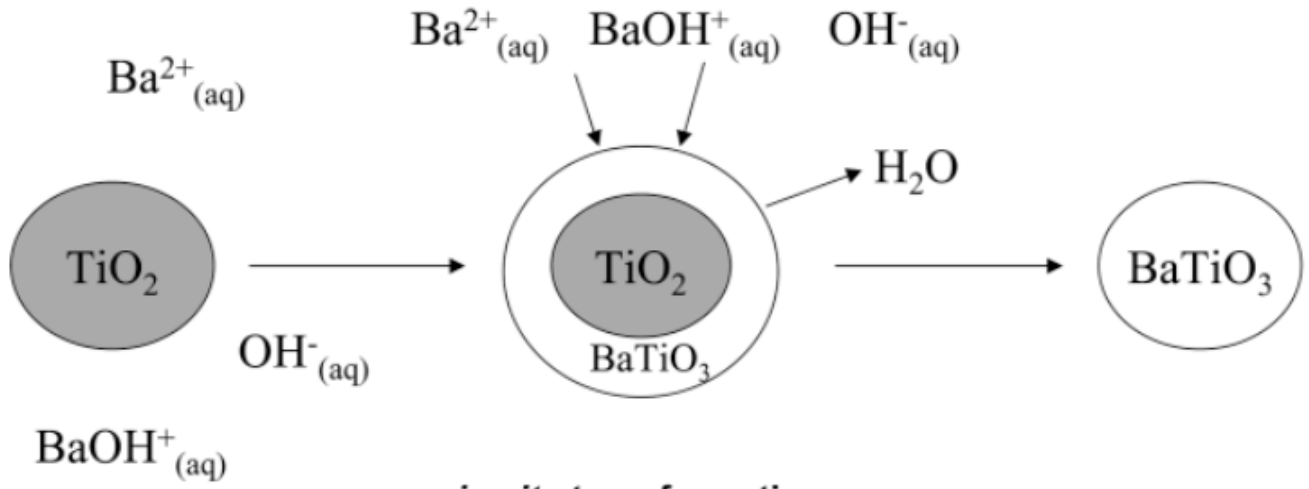

***in situ* transformation**

B

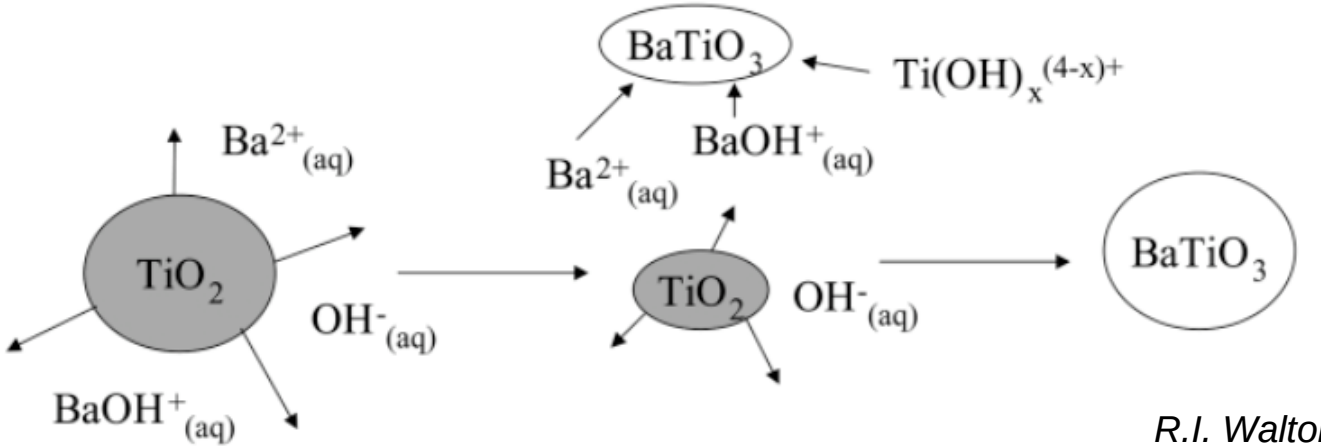

dissolution-precipitation

R.I. Walton, Chem. Soc. Rev. 31 (2002) 230–238.

Dissolution - solvation

Table 1.1 Hydration enthalpies (kJ mol^{-1}, 25 °C) and ionic radii (Å) of a few ions [16]

Ion	$-\Delta H°$	Radius	Ion	$-\Delta H°$	Radius
H^+	1100	–			
Li^+	522	0.78	Cr^{2+}	1930	0.80
Cs^+	285	1.65	Fe^{2+}	1956	0.83
Mg^{2+}	1940	0.78	Ni^{2+}	2120	0.78
Ba^{2+}	1320	1.43	Cr^{3+}	4620	0.65
Al^{3+}	4700	0.57	Fe^{3+}	4450	0.67

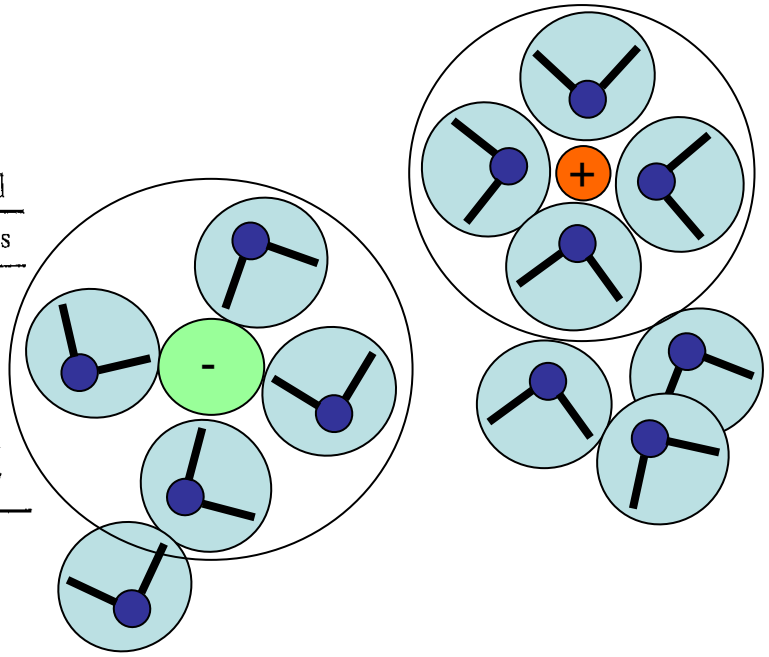

$[M(OH_2)_6]^{2+}$ M= Mg, Ca, Cd, Hg, Pb, V, Cr, Mn, Fe, Co, Ni, Cu, Zn

$[M(OH_2)_8]^{2+}$ M= Sr

$[M(OH_2)_6]^{3+}$ M= Al, V, Cr, Mn, Fe

Ions with a charge higher than three undergo hydrolysis

Acid-base properties of coordinated water molecules

$$[M(OH_2)]^{z+} \xrightleftharpoons{H_2O} [M(OH)]^{(z-1)+} + H^+_{aq} \xrightleftharpoons{H_2O} [M\text{-}O]^{(z-2)+} + 2\,H^+_{aq}$$

aquo	hydroxo	oxo
pH<7, $z \leq 4$	pH>7, $z \leq 4$	$z > 4$

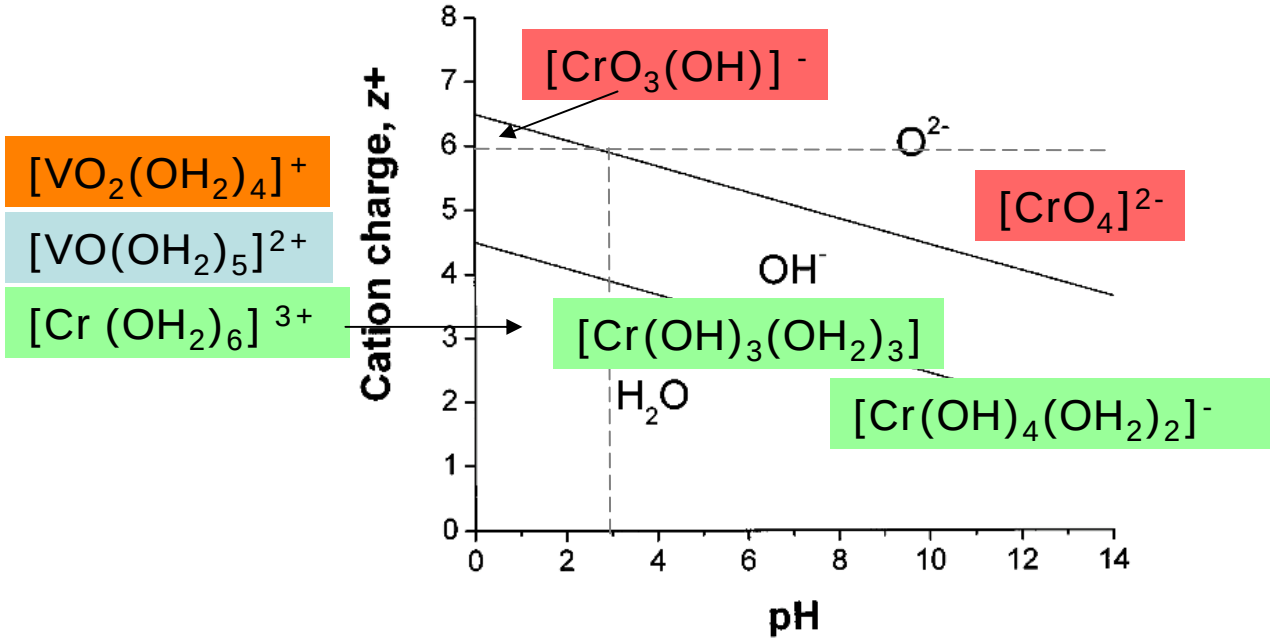

Small cations of high formal charge (z>4) form π bonds (V:r=0.54Å)

Figure 18. Relationship between charge, pH, and hydrolysis equilibrium of cations. (Reprinted with permission from ref 254. Copyright 1972 David Kepert.)

B.L. Cushing et al., Chem. Rev. 104 (2004) 3893-3946.

Solubility of TiO_2 under hydrothermal conditions

Ti(IV) hydrolysis constants derived from rutile solubility measurements made from 100 to 300°C

*Kevin G. Knauss *, Michael J. Dibley, William L. Bourcier, Henry F. Shaw*
Applied Geochemistry 16 (2001) 1115-1128.

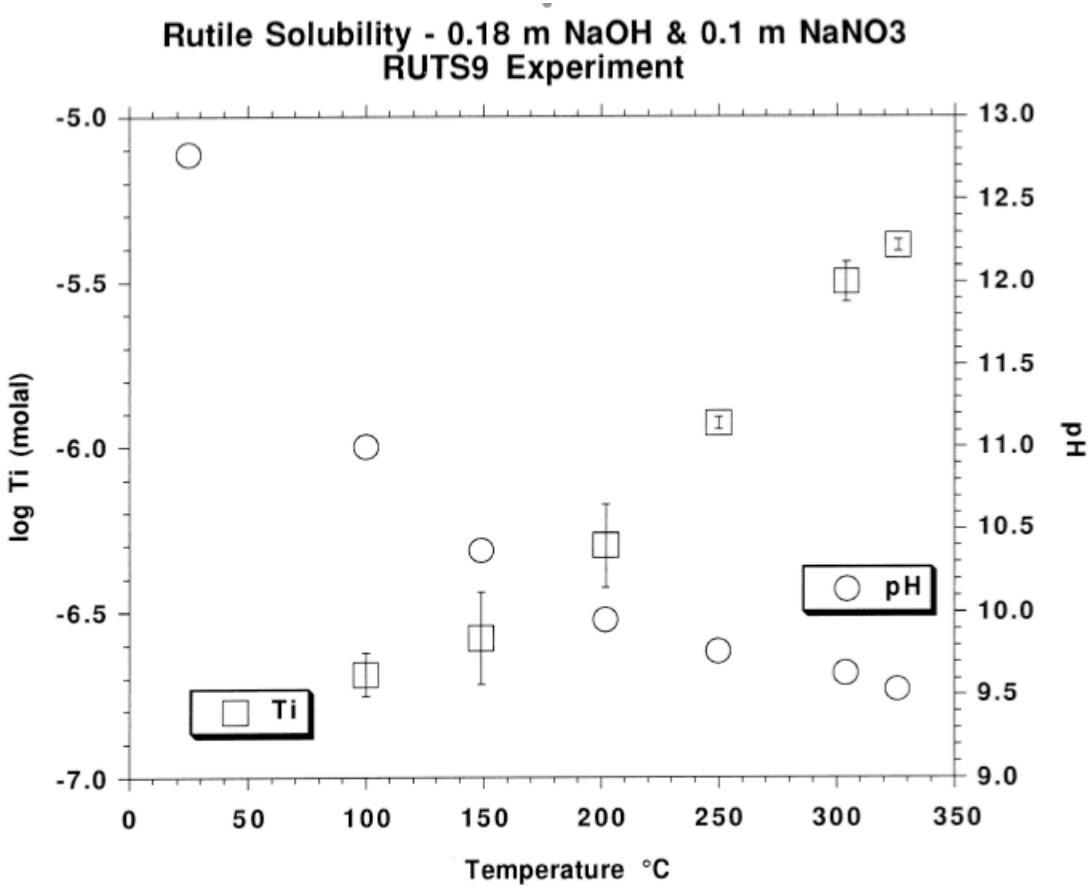

Fig. 3. Plot of Ti concentration and calculated pH from RUTS9 experiment (0.18 m NaOH and 0.1 m $NaNO_3$).

Solubility of TiO_2 under hydrothermal conditions

Ti(IV) hydrolysis constants derived from rutile solubility measurements made from 100 to 300°C

*Kevin G. Knauss *, Michael J. Dibley, William L. Bourcier, Henry F. Shaw*
Applied Geochemistry 16 (2001) 1115-1128.

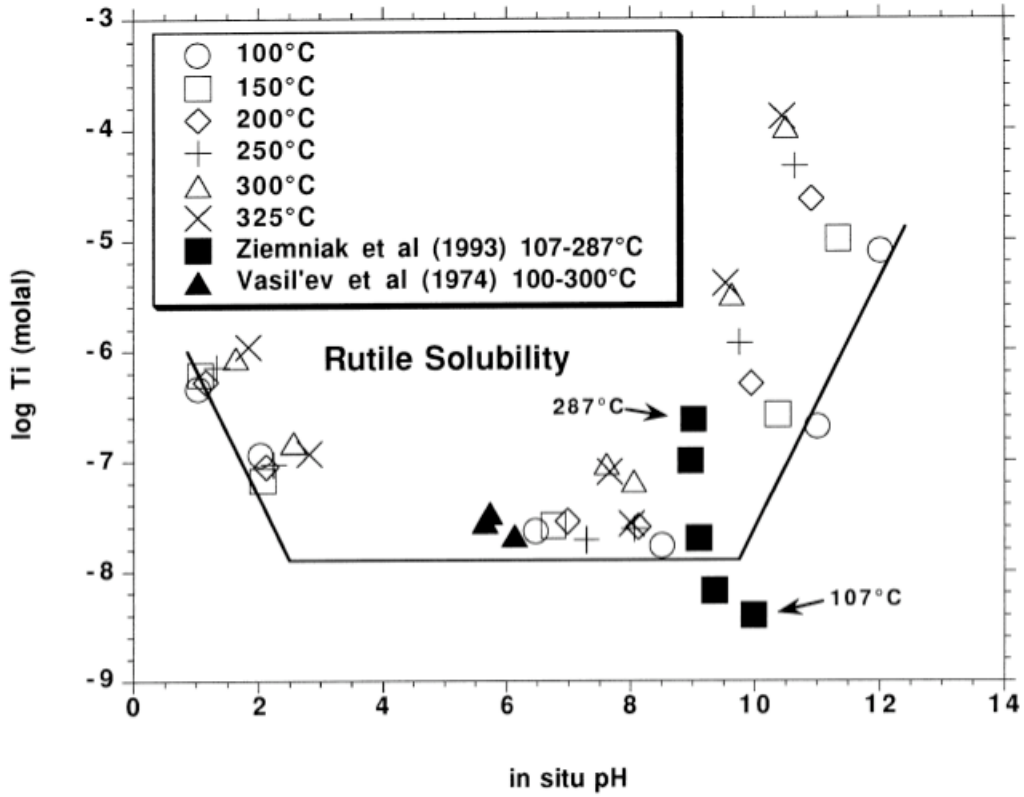

Fig. 4. Summary plot of Ti concentration data from this work as well as those from Ziemniak et al. (1993) and Vasil'ev et al. (1974).

Polycondensation in aqueous solution

Addition of a base to an aquo complex (polycations)

$[Al(OH_2)_6]^{3+} + 3\ OH^- \rightarrow Al(OH)_3 + 6\ H_2O$

$13\ [Al(OH_2)_6]^{3+} + 32\ OH^- \rightarrow [Al_{13}O_4(OH)_{24}(OH_2)_{12}]^{7+} + 70\ H_2O$

Addition of an acid to an oxo complex (polyanions)

$[SiO_2(OH_2)_2]^{2-} + 2\ H^+ \rightarrow SiO_2 + 2\ H_2O$

$4\ [SiO_2(OH_2)_2]^{2-} + 4\ H^+ \rightarrow [Si_4O_{12}]^{4-} + 4\ H_2O$

Transition metal ions often change the coordination

$12\ [WO_4]^{2-} + 18\ H_3O^+ \rightarrow [H_2W_{12}O_{40}]^{6-} + 26\ H_2O$

Initiation → Propagation → Termination

Initiation (hydroxylation)

$$[M\text{-}O]^- + H_3O^+ \longrightarrow M\text{-}OH + H_2O \longleftarrow [M\text{-}OH_2]^+ + HO^-$$

precursor

Propagation (nucleophilic addition/substitution)

$$M\text{-}OH + M\text{-}OH_2 \longrightarrow M\text{-}OH\text{-}M + H_2O$$

Olation
Oligomeric species: Polycations
Reaction leading to a hydroxy bridge

$$M\text{-}OH + M\text{-}OH \longrightarrow M\text{—}\overset{\overset{H}{|}}{O}\text{—}M\text{—}OH \longrightarrow M\text{-}O\text{-}M + H_2O$$

Oxolation
Oligomeric species: Polyanions
Reaction leading to an oxo bridge

Termination

- Condensation of cationic or anionic hydroxylated complexes limited
- The formation of a solid requires the presence of zero-charge complexes

Hydrothermal zeolite synthesis

$$T{-}OH + {}^{-}O{-}T \rightleftharpoons T{-}O{-}T + OH^{-}$$

$$T{-}OH + HO{-}T \rightleftharpoons T{-}O{-}T + H_2O$$

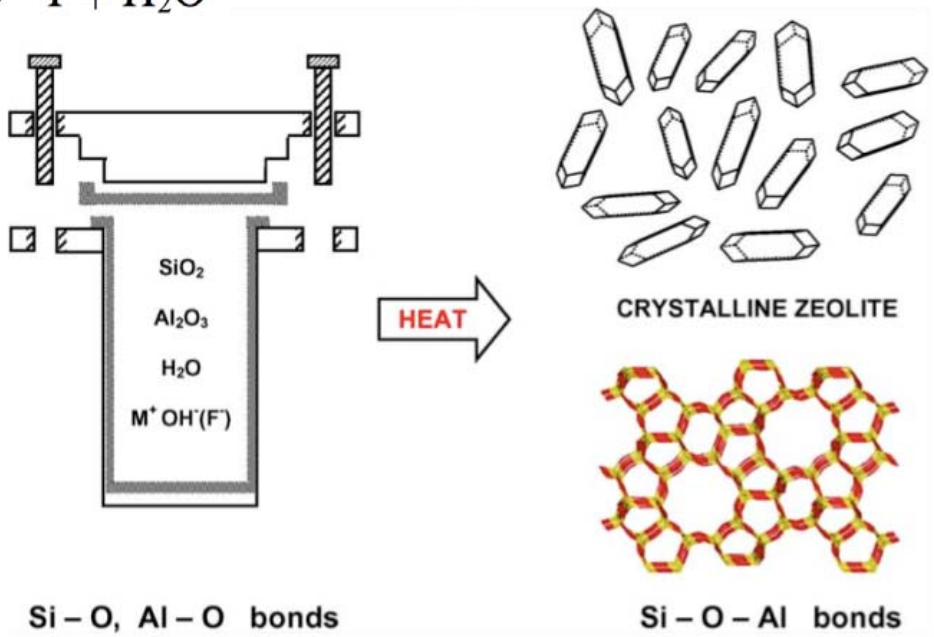

C.S. Cundy, P.A. Cox Microporous and Mesoporous Materials 82 (2005) 1-78.

Fig. 1. Hydrothermal zeolite synthesis. The starting materials (Si—O and Al—O bonds) are converted by an aqueous mineralising medium (OH^- and/or F^-) into the crystalline product (Si—O—Al bonds) whose microporosity is defined by the crystal structure.

Experimental procedure

1. Mixing amorphous reactants containing Si and Al in a basic medium
2. Heating (often) above 100 °C in a sealed autoclave.
3. Isolation of the crystalline zeolite product

Hydrothermal zeolite synthesis

C.S. Cundy, P.A. Cox / Microporous and Mesoporous Materials 82 (2005) 1–78

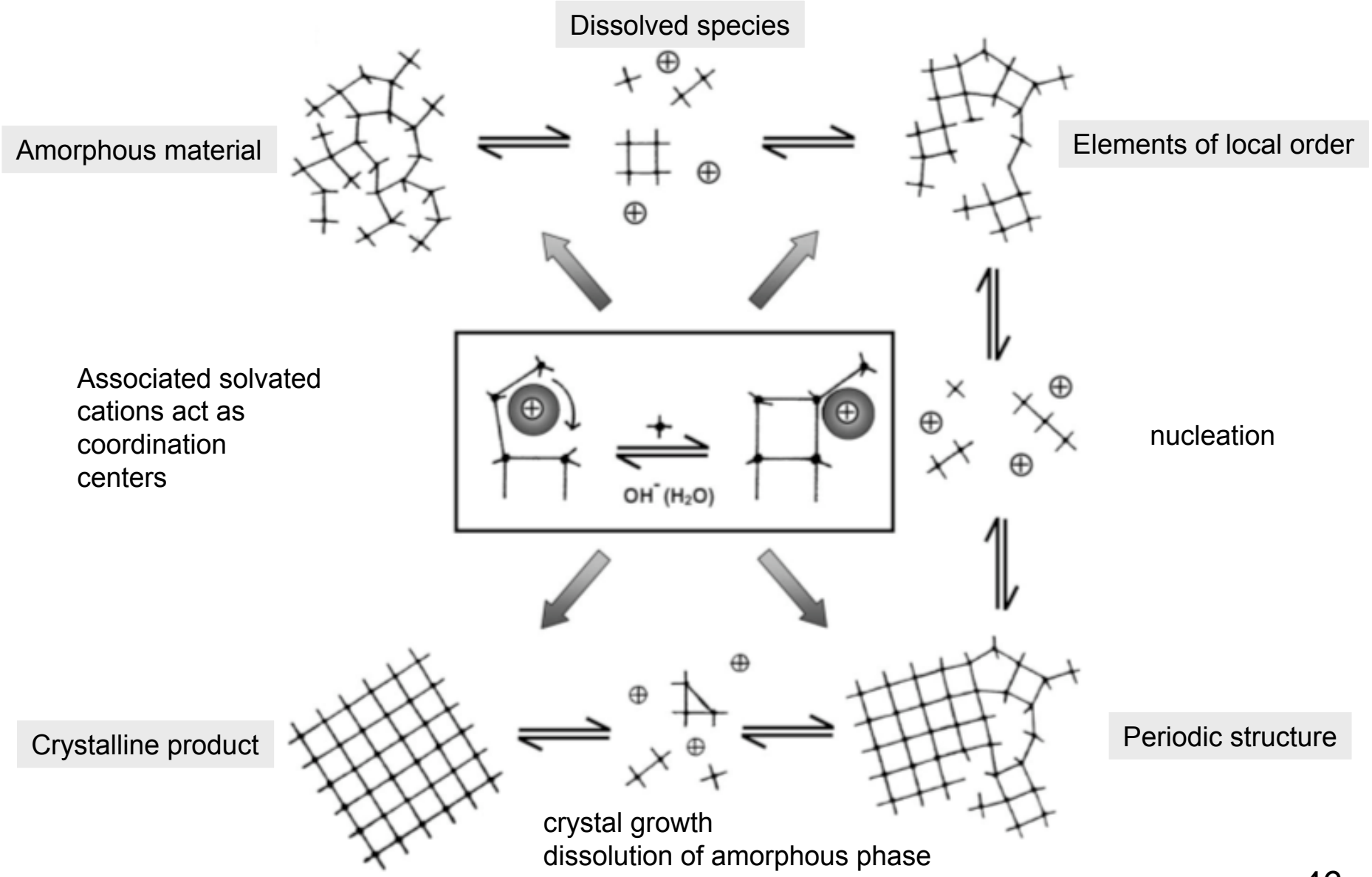

Matching between ZSM-18 and the triquat template molecule used in ist synthesis

Templates

- „space fillers“
- Structure directing agents
- True templates

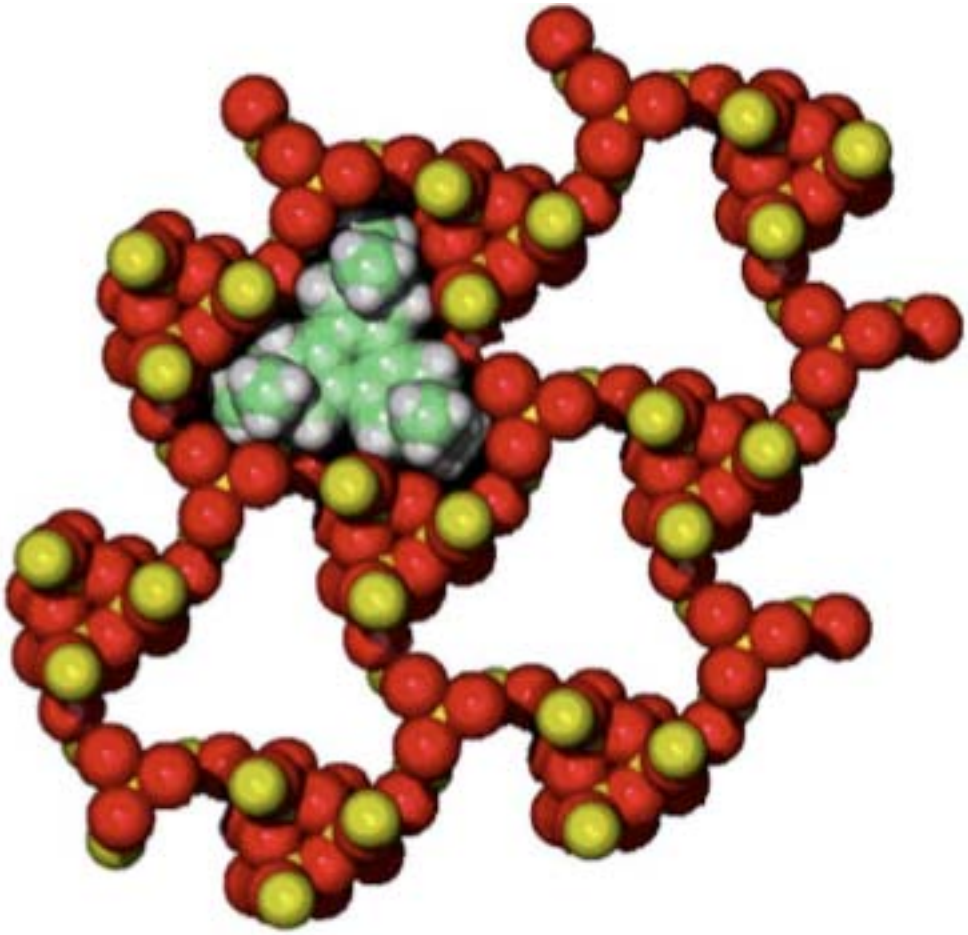

C.S. Cundy, P.A. Cox / Microporous and Mesoporous Materials 82 (2005) 1-78.

Transition metal ions in aqueous solution

$2[VO_4]^{3-} + 2H^+ \rightarrow [V_2O_7]^{4-} + H_2O$

$4[VO_4]^{3-} + 8H^+ \rightarrow [V_4O_{12}]^{4-} + 4H_2O$

In diluted solution:

V_2O_5 precursor

$[VO(OH)_3(OH_2)_2]$

$[VO_2(OH)(OH_2)_3]$

$10[VO_4]^{3-} + 25H^+ \rightarrow [HV_{10}O_{28}]^{5-} + 12H_2O$

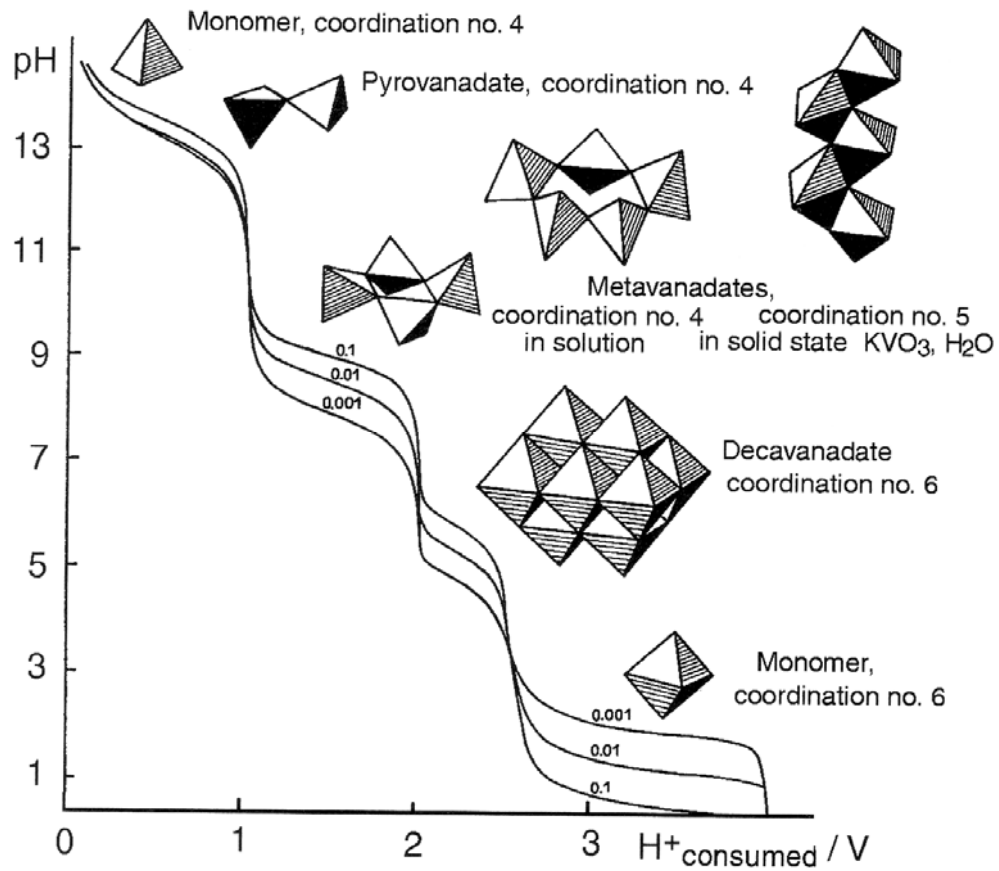

$[H_2V_{10}O_{28}]^{4-} + 14H_3O^+ + 18H_2O \rightarrow 10\ [VO_2(H_2O)_4]^+$

vanadic cation

Hydrothermal synthesis of vanadium oxide

Scroll-like morphology of the products of the two- day hydrothermal treatment of dodecylamine-intercalated V_2O_5

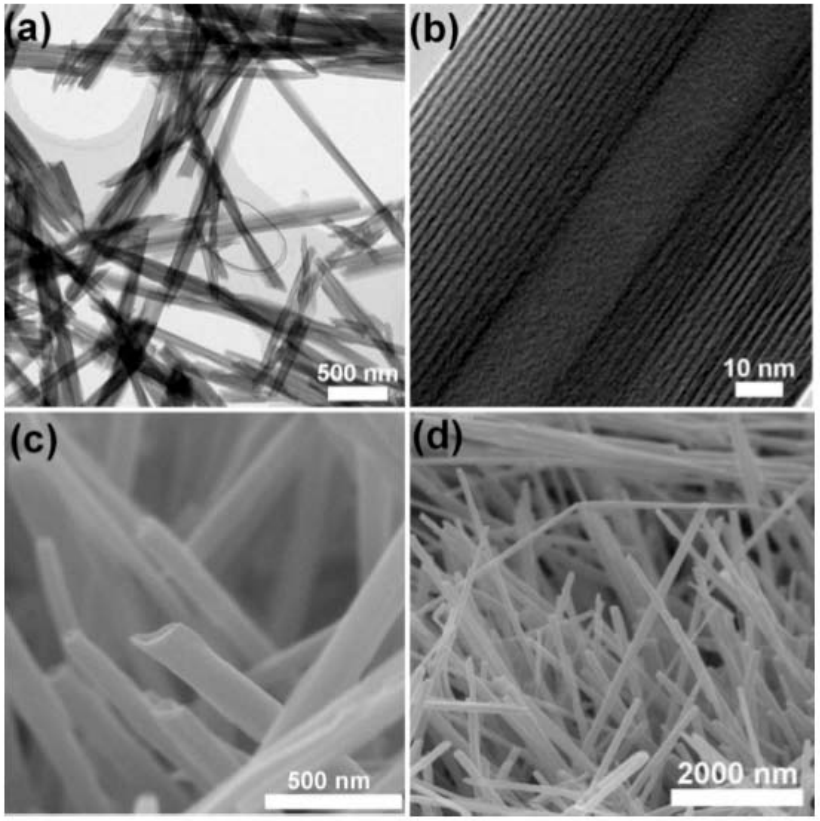

Figure 2. (a, b) TEM and (c, d) SEM images of hydrothermally prepared $V_2O_{5-\delta}$ nanoscrolls prepared for two days. The average diameter of is 125 nm, whereas the average length stretches several micrometers long (typically 5 μm). Regular interlayer spacings of ~2 nm are evide magnification TEM images, and there are typically 20 layers per scroll.

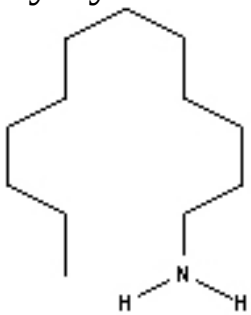

Vanadium oxide nanorods for Li-ion battery applications by template-free hydrothermal synthesis at 180°C/15 d

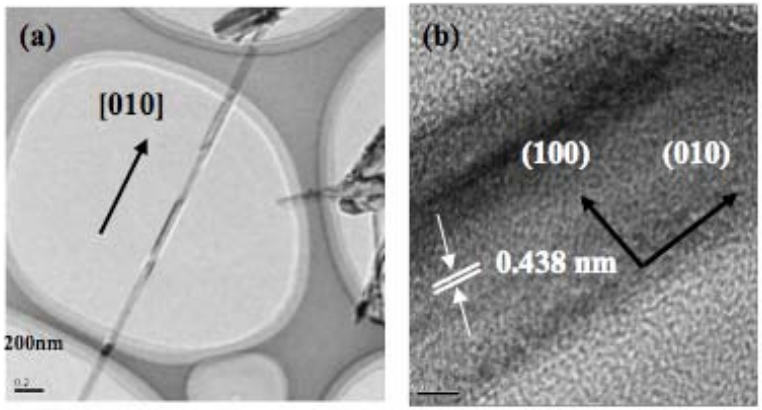

Figure 4. TEM images of the vanadium oxide nanorods: (a) low magnification and (b) HRTEM image.

S.A. Corr, et al., Chem. Mater. 20 (2008) 6396-6404.

Ch. V. Subba Reddy et al., Journal of the Electrochemical Society, 155 (2008) A599-A602.

Transition metal ions in aqueous solution

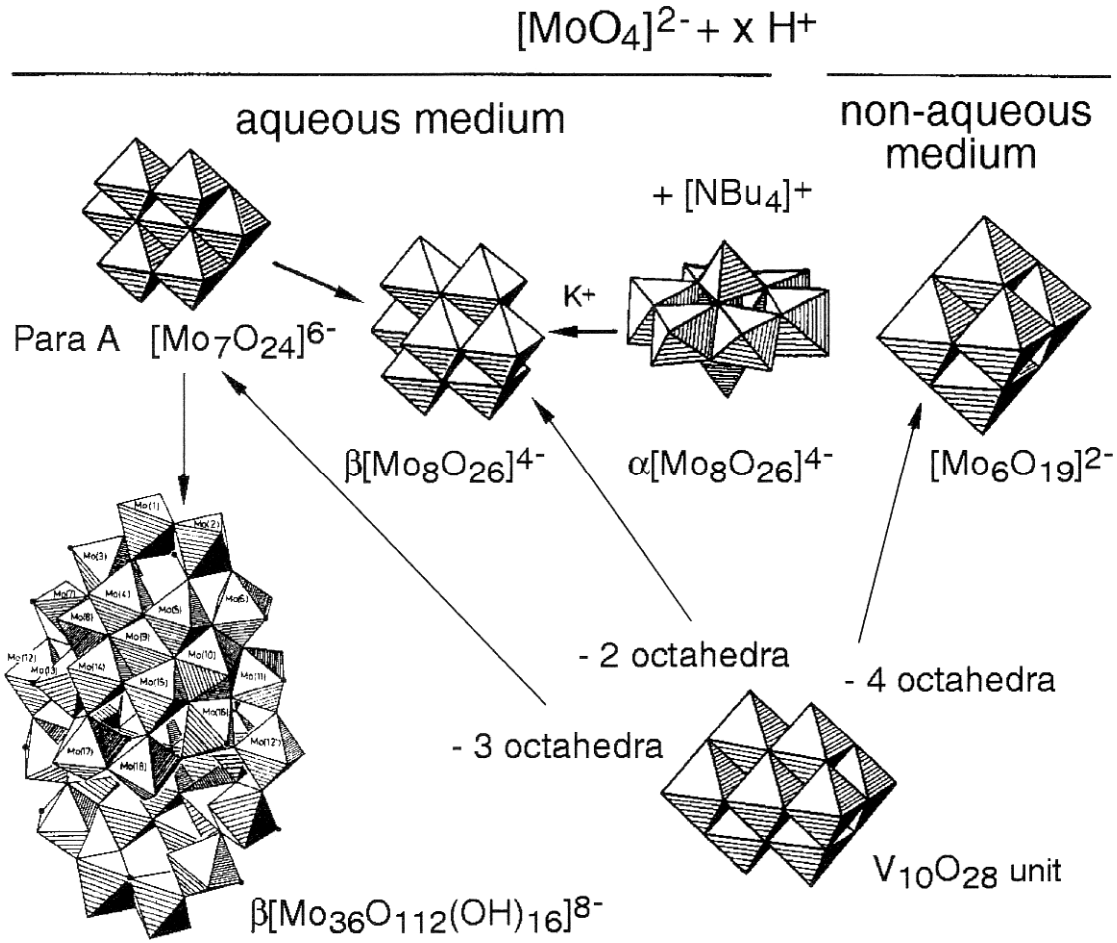

HTS, 110°C, molybdic acid solution

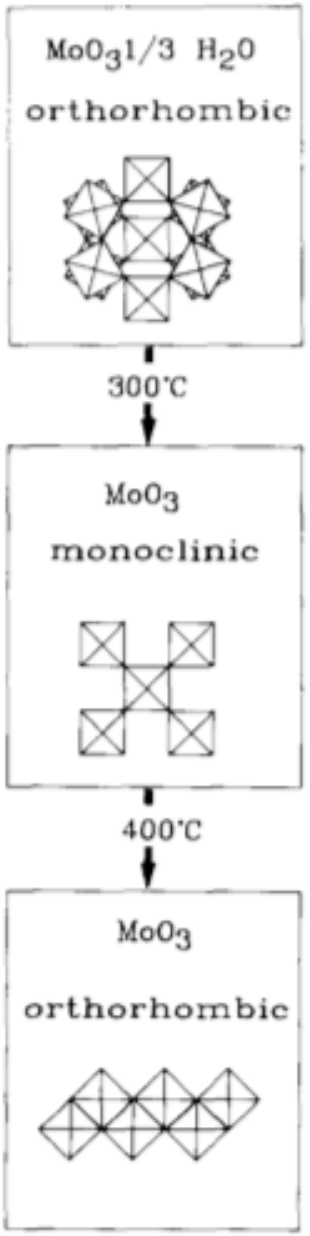

F. Harb et al., Solid Statc Ionics 32/33 (1989) 84-90.

Hydrothermal synthesis of MoV oxide

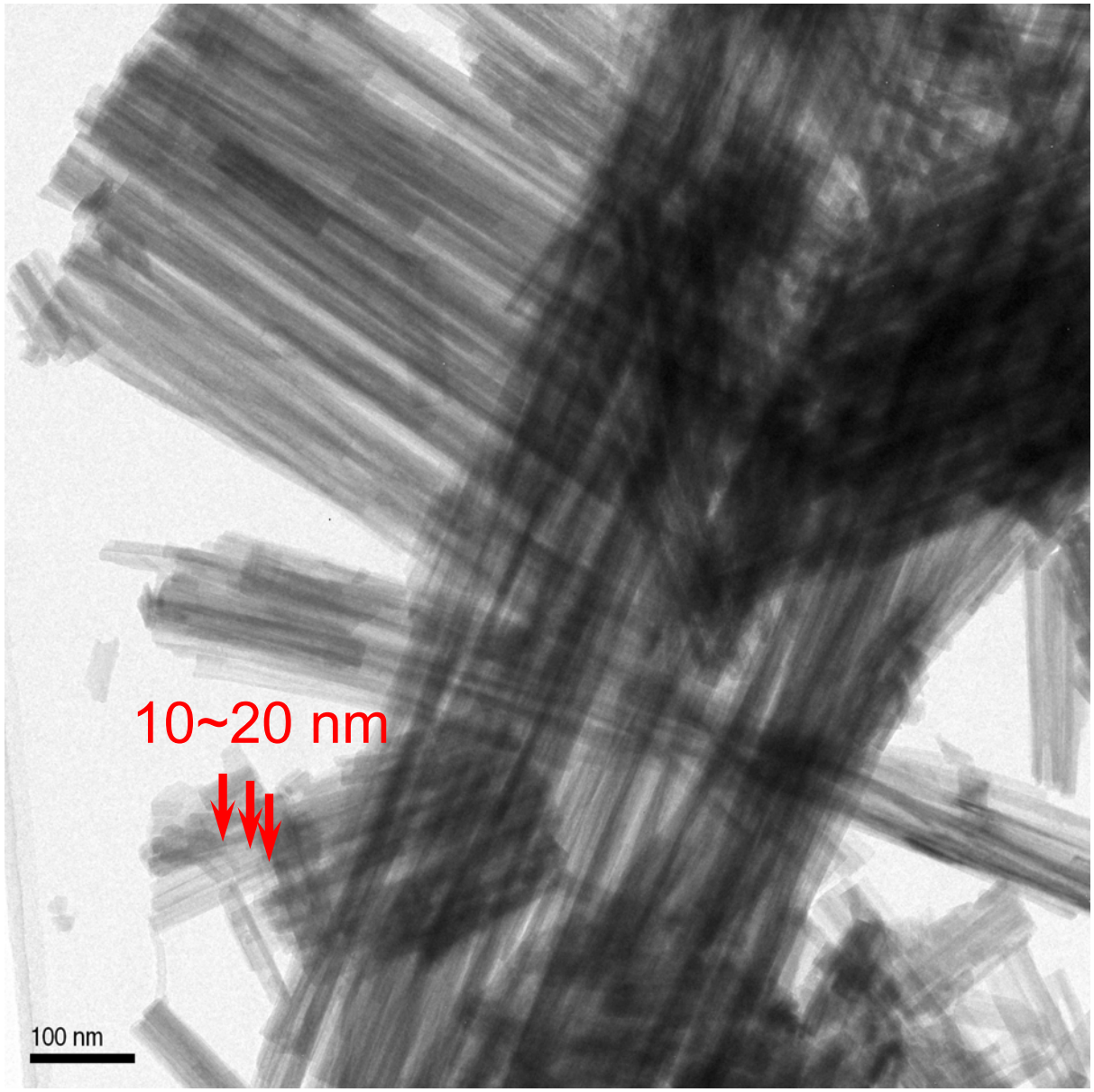

BET surface area

#6142: 69.21m²/g

#6274: 79.41m²/g

Synthesis of M1 (MoVTeNb mixed oxide)

Phase formation by dissolution-precipitation mechanism

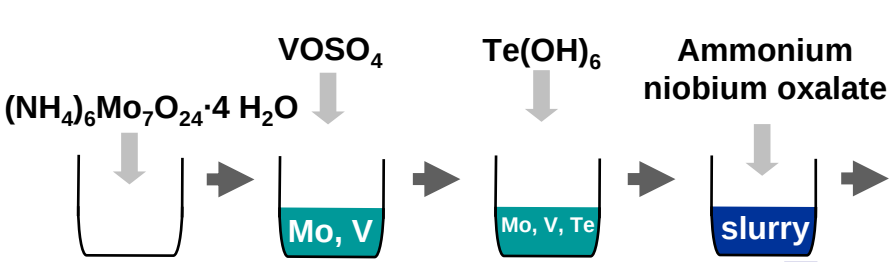

V= 300 ml Teflon

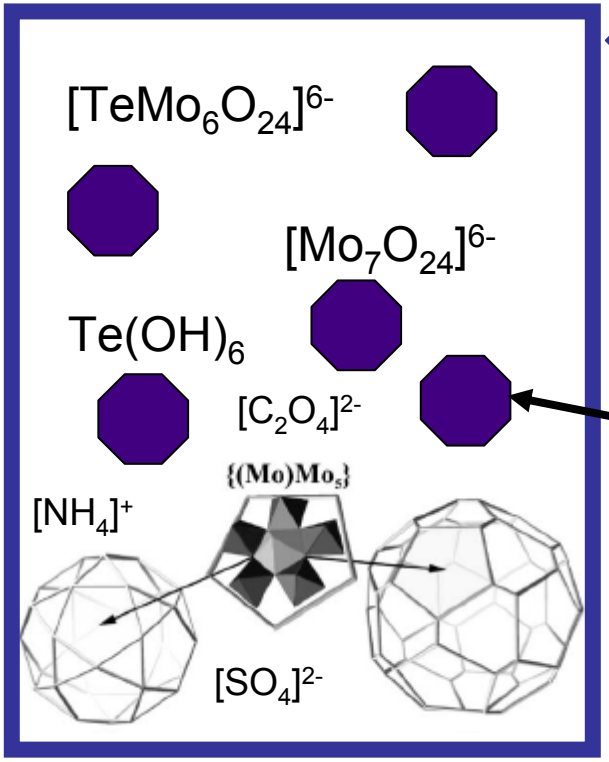

Raman
UV-vis
SEM-EDX

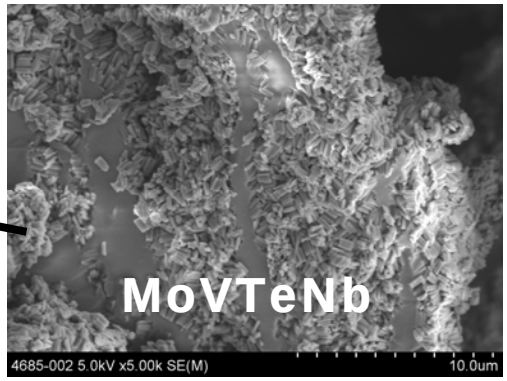

Starting suspension: inhomogeneous slurry that contains an amorphous solid

Mo and MoV clusters:
A. Müller, S. Roy,
Coordination Chemistry Reviews
245 (2003) 153–166.

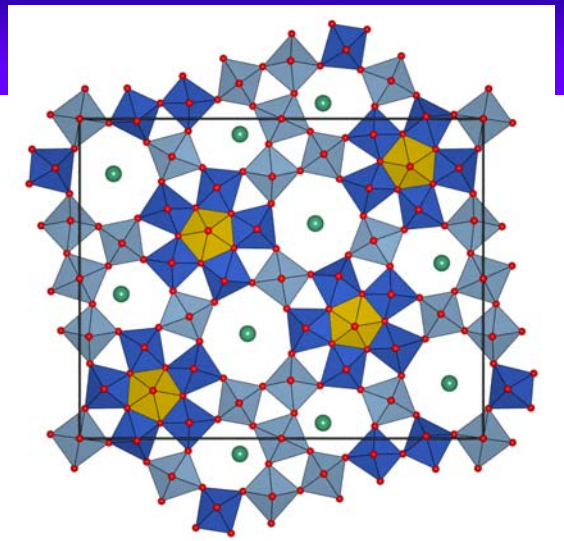

a=21.1 Å

b=26.6 Å

Synthesis of M1 (MoVTeNb mixed oxide)

V= 300 ml
teflon

- T = 383-448K
- $t_{synt.}$ = 96h
- inert gas = N_2

Variation of the synthesis temperature at t=96h

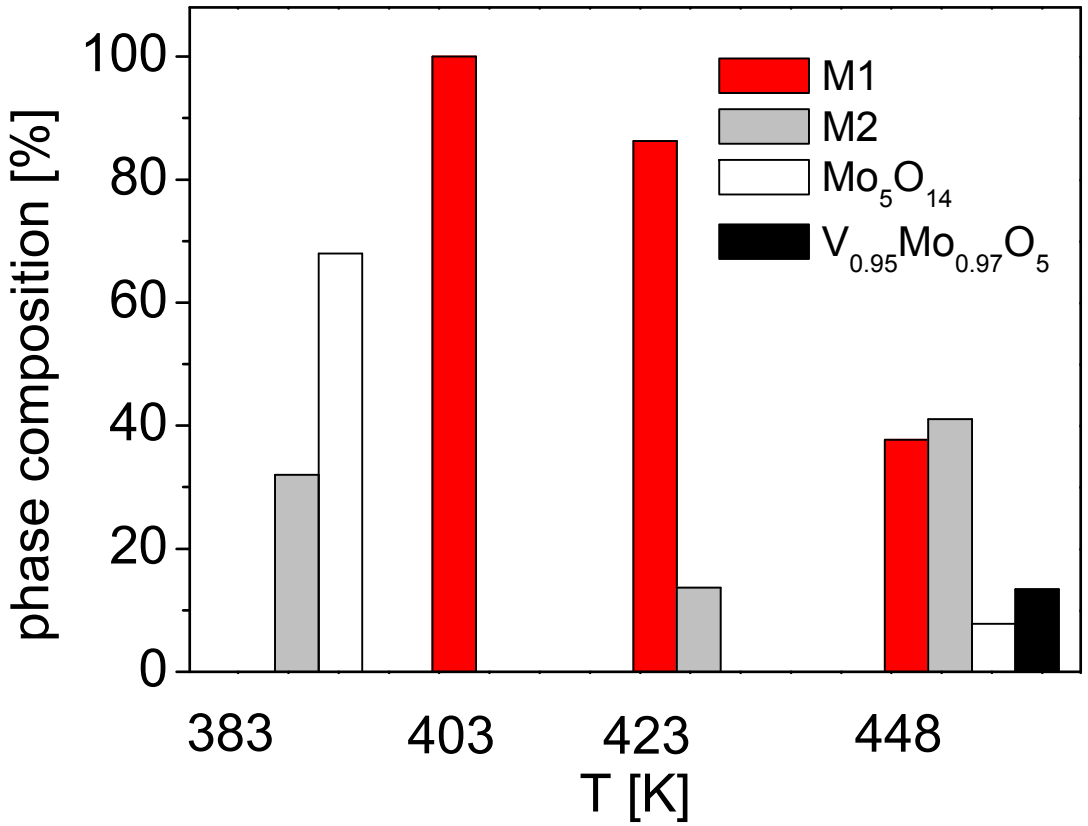

Synthesis of M1 (MoVTeNb mixed oxide)

XRD of amorphous precursor after hydrothermal synthesis

phases after crystallization / %

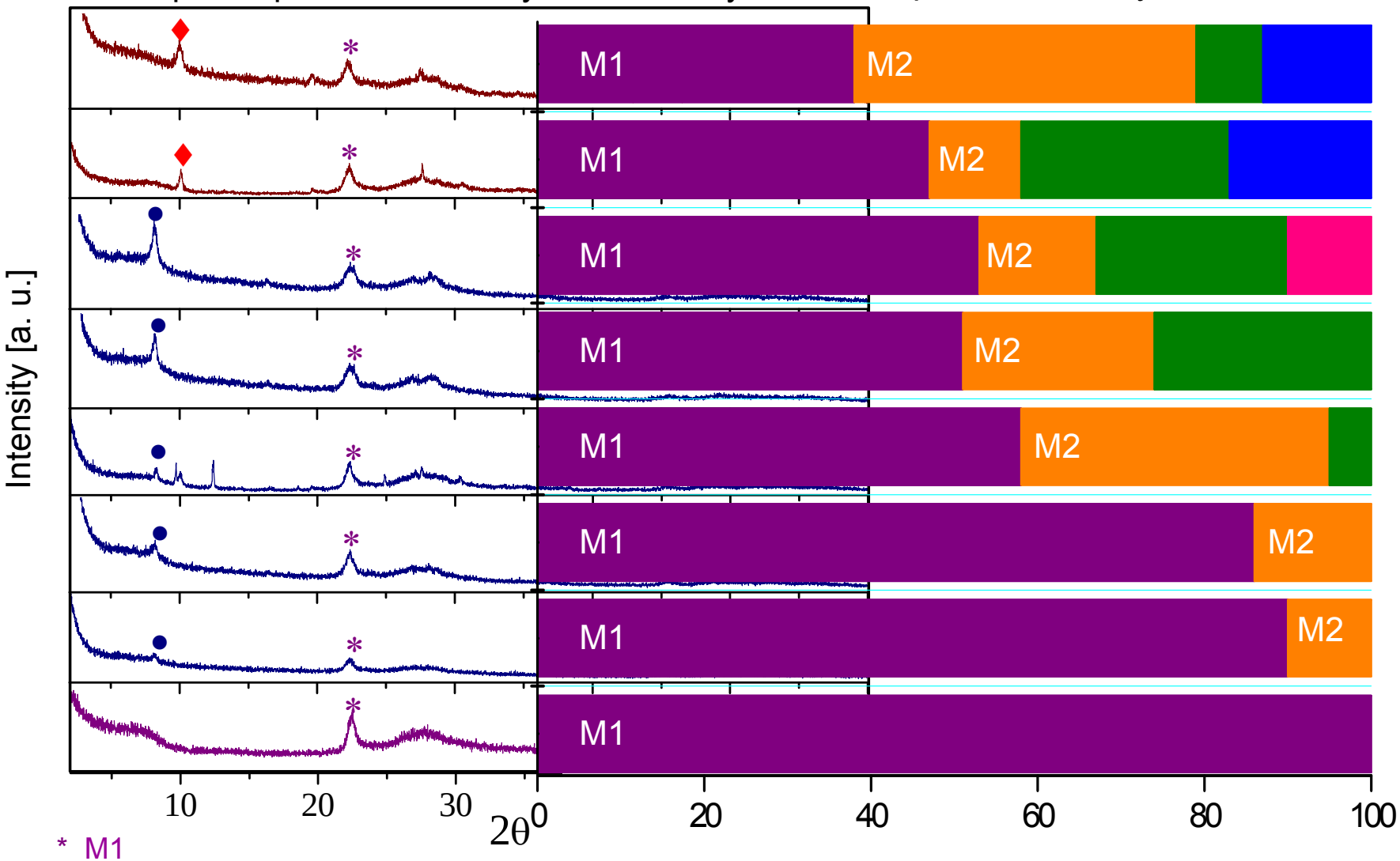

* M1

● $(NH_4)_8(V_{19}O_{41}(OH)_9)(H_2O)_{11}$ [ICSD 063213]

♦ $(NH_4)_6Mo_8O_{27}\cdot 4H_2O$ [ICSD 2017]

M_5O_{14} (M=Mo,V,Nb)

$TeMo_5O_{16}$

$V_{0.95}Mo_{0.97}O_5$

Reaction of solid oxides with superheated steam

O. Glemser, U. Stöcker, H.G. Wendlandt, Ber. Bunsenges. 70 (1966) 1129.

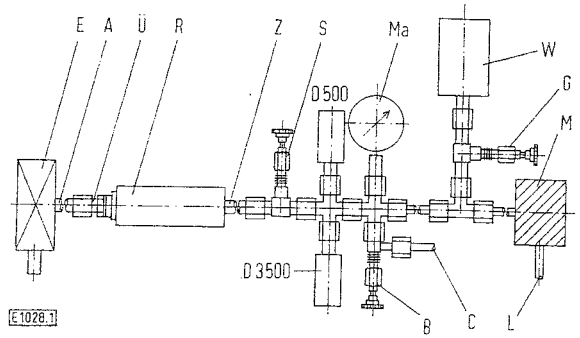

Abb. 1
Mitführungsapparatur für Drücke bis zu 3000 atm
W = Windkessel, C = Verbindung zur Stahlflasche mit Stickstoff, B, G, S = Absperrventile, E = Entspannungsventil, L = Vorratsbehälter mit Wasser, M = Membrandosierungspumpe, D500, D3500 = Druckaufnehmer für 500 bzw. 3500 kg/cm², Z = Zuführung zur Reaktionszelle, R = Reaktionszelle, Ü = Überführungsteil, A = Kondensationsrohr, Ma = Manometer

Tabelle 3
Auftretende Spezies bei der Reaktion $MoO_{3\,fest} + H_2O_{Gas}$

Dichtebereich	
I (bei etwa 0,05 g/cm³)	$MoO_{3(fest)} + H_2O_a \rightleftharpoons MoO_2(OH)_{2\,(a)}$
II (von 0,1 bis 0,55 g/cm³)	$7\,MoO_{3(fest)} + 3\,H_2O \rightleftharpoons Mo_7O_{18}(OH)_{6\,(a)}$ [30]
III (ab 0,55 g/cm³)	$MoO_{3(fest)} + H_2O_{(a)} \rightleftharpoons MoO_2(OH)_{2\,(a)}$ [31]

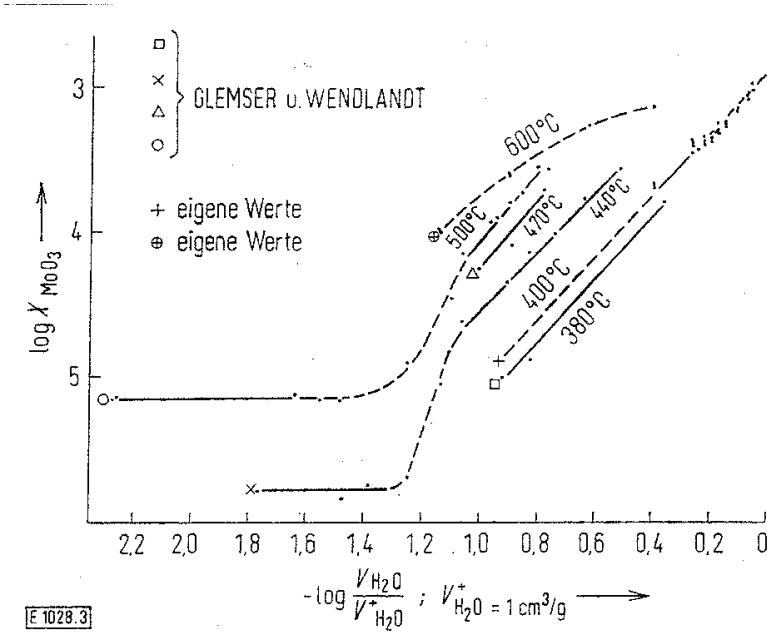

Abb. 3
Löslichkeit von MoO_3 in H_2O bei verschiedenen Temperaturen und Drucken

Synthesis of MoVTeNb oxide

Hydrothermal synthesis under mild conditions

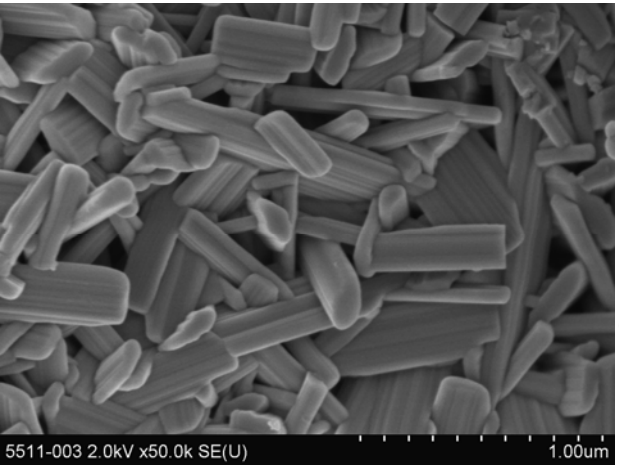

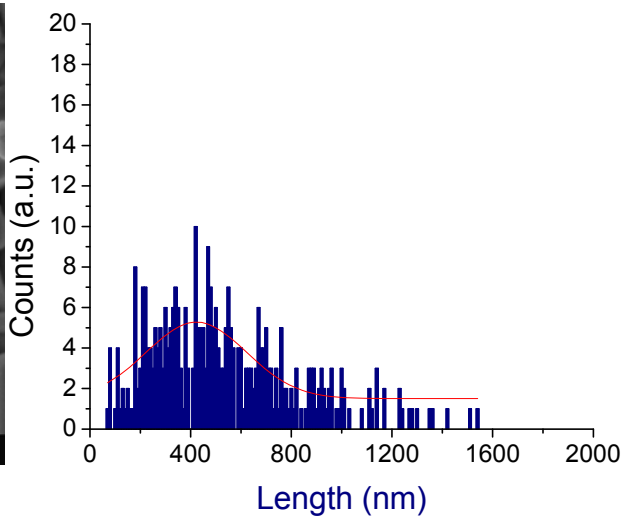

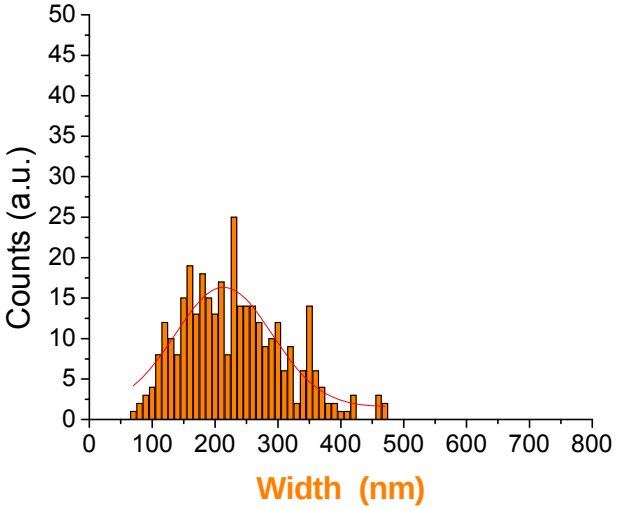

Hydrothermal synthesis in superheated water vapour

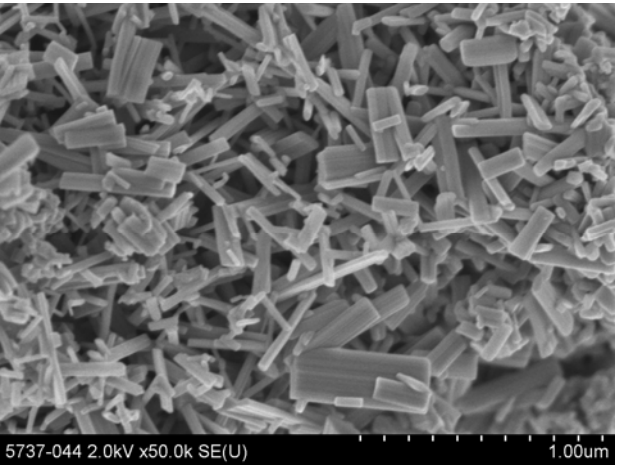

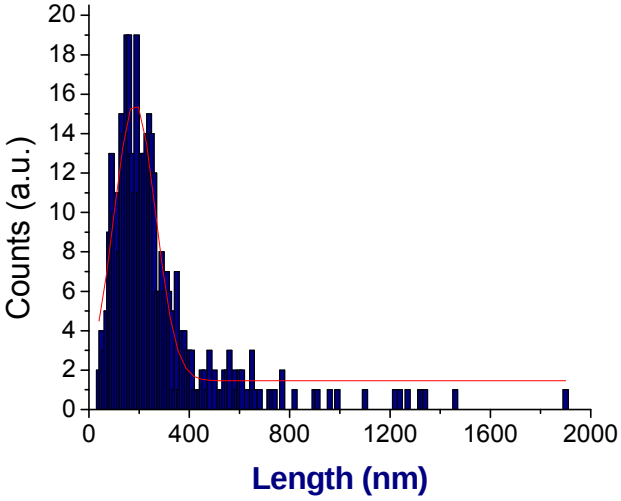

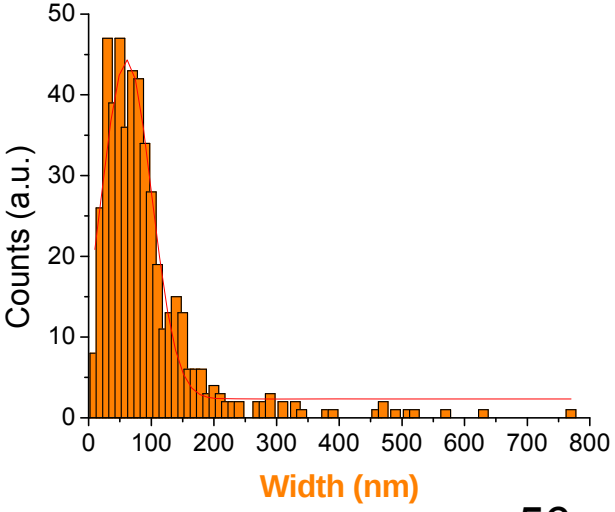

Synthesis under supercritical conditions

Methods for the preparation of nanoparticles

- Particles with one dimension smaller than 200-100 nm
- Surface properties become relevant with respect to volume properties

- Precipitation
  - Rapid expansion of supercritical solutions (RESS)
  - Rapid expansion of a supercritical solution into a liquid solvent (RESOLV)
  - Supercritical anti-solvent precipitation (SAS)

- Supercritical solvothermal synthesis

- Supercritical drying

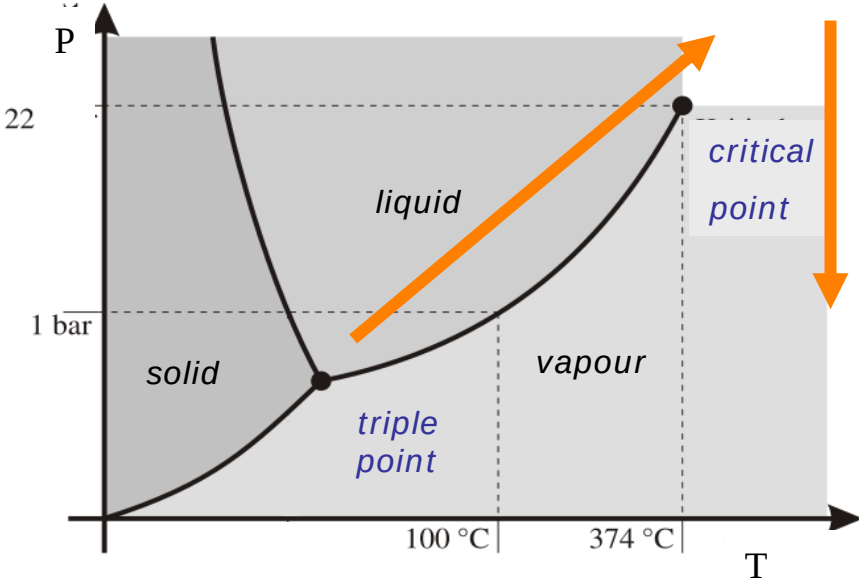

Other solvents

Table 1. Critical point parameters of solvents.[5, 10]

Solvent	T /K	P /MPa	ρ /kg m^{-3}
C_2H_4	282.1	5.041	214
Xe	289.5	5.840	1110
CO_2	303.9	7.375	468
C_2H_6	305.2	4.884	203
N_2O	309.4	7.255	452
NH_3	405.3	11.350	235
C_2H_5OH	513.7	6.137	276
H_2O	646.9	22.060	322

Reducing T and p

Catalyst	Fluid	T / K	p / MPa	Phase composition
$MoVTeNbO_x$	H_2O	773	20	M1
$MoVTeNbO_x$	CO_2	573	6	M1

Microwave assisted hydrothermal synthesis

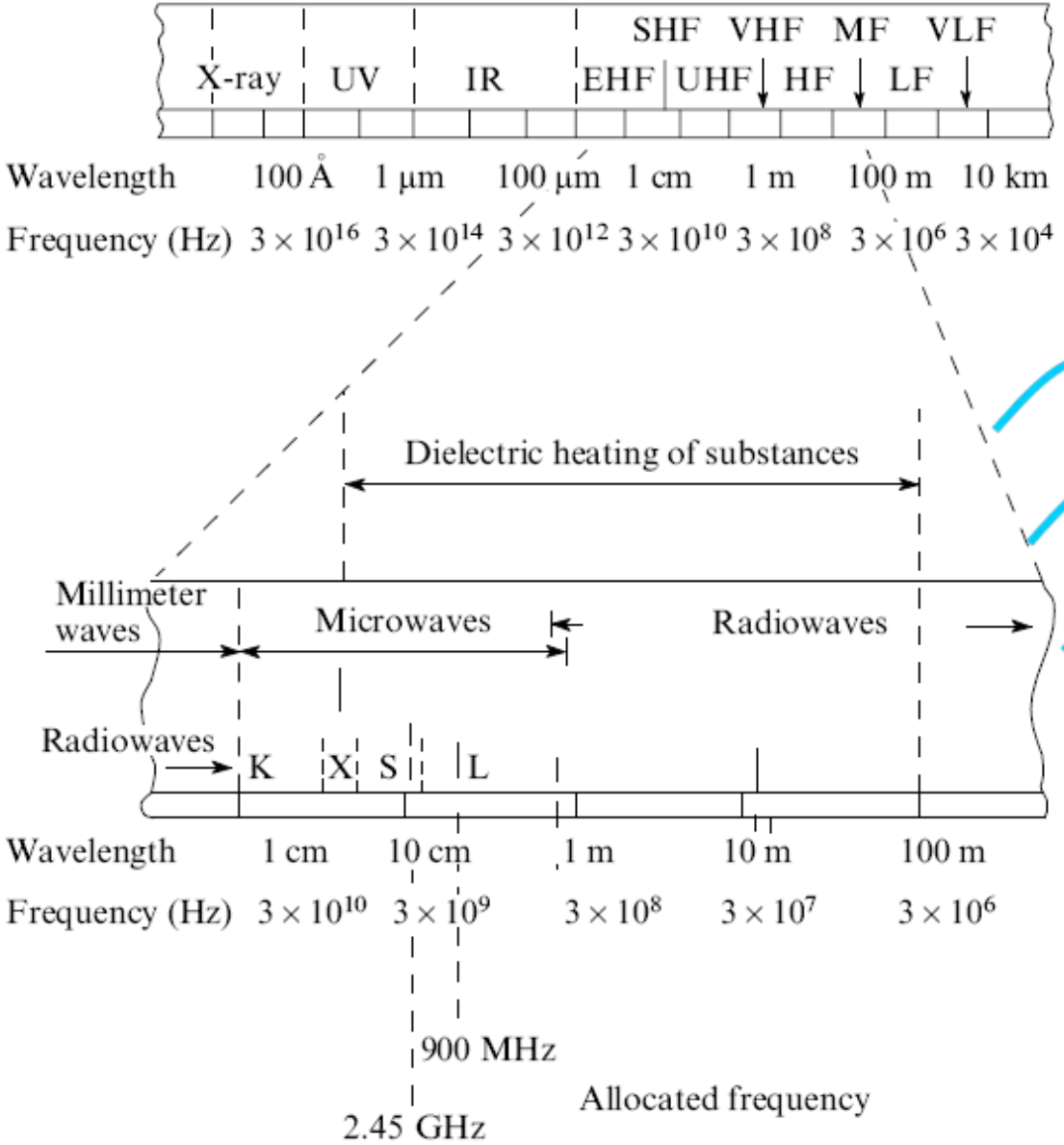

A. S. Vanetsev, Yu.D. Tretyakov, Russ. Chem. Rev. 76 (2007) 397-413.

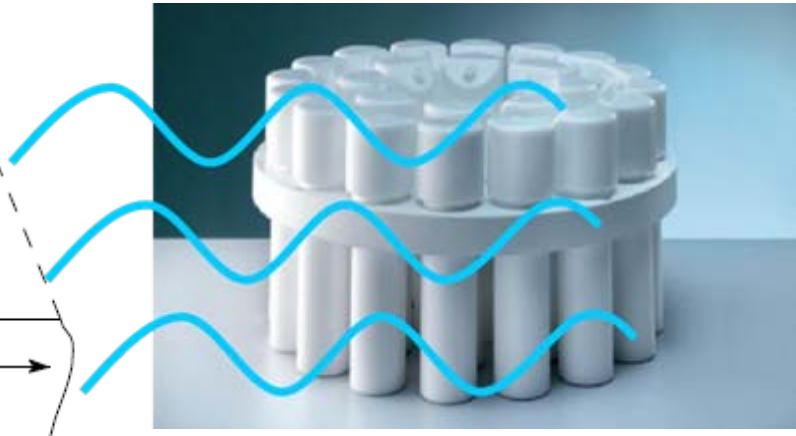

Domestic and laboratory microwave ovens:

ν= 2.45 GHz ($\lambda \approx$ 12.2 cm)

ν = 915 MHz ($\lambda \approx$ 32.7 cm)

Interaction of microwave radiation with matter

1. **Electronic and ionic conductivity**
- Insulators are transparent
- Conducting materials reflect the microwave radiation (destroy the magnetron by overheating)
2. **Dielectric permittivity and dielectric loss factor (absorption capacity)**
- The substances should contain mobile dipoles (high dipole moment) or ionic conductivity
- The more efficiently the sample absorbs, the smaller is the volume that can be heated
- Dielectric properties depend on temperature
3. **Heat conductivity to avoid „hot spots“**

Table 7. Dielectric permittivity (real and imaginary parts), skin depth, and loss tangent for various media at 2.45 GHz (12.24 cm wavelength).

Medium	Temperature [°C]	Dielectric permittivity (real part) ε'	Dielectric permittivity (imaginary part) ε''	Skin depth δ_s [cm]	Loss tangent $\tan\delta$	Reference
ethylene glycol	25	37	49.95	0.55	1.35	[137]
water	25	78	10.33	3.33	0.13	[137]
silicalite solution	25	49.5	20.13	1.38	0.407	this work
beta solution	25	43.4	77.1	0.41	1.78	this work
NaY solution (AS-40 colloidal silica)	25	37	147.5	0.26	3.9	this work
NaY solution (Aerosil 200 fumed silica)	25	48.7	137.25	0.28	2.82	this work
SBA-15 solution (BASF P-123)	25	46.59	331.13	0.16	7.11	this work

G. A. Tompsett et al., ChemPhysChem 7 (2006) 296 – 319.

Microwave assisted hydrothermal synthesis

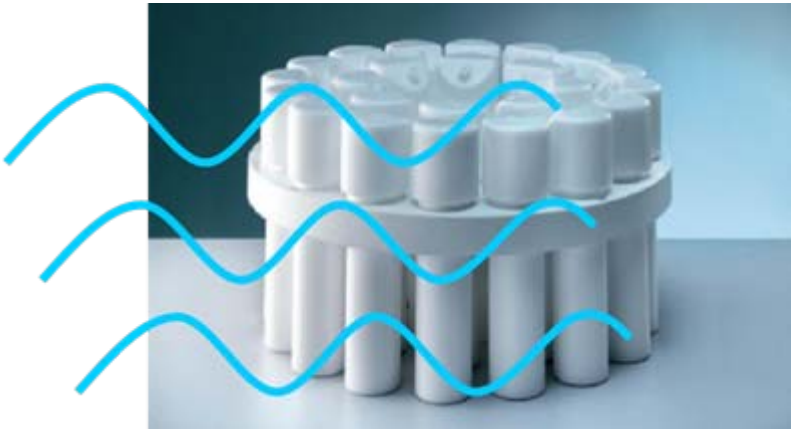

M1 synthesis by a factor of ca. 10 faster

- High rates of phase formation
- Processes in the microwave field caused by possible acceleration of nucleation due to „non-thermal“ effects

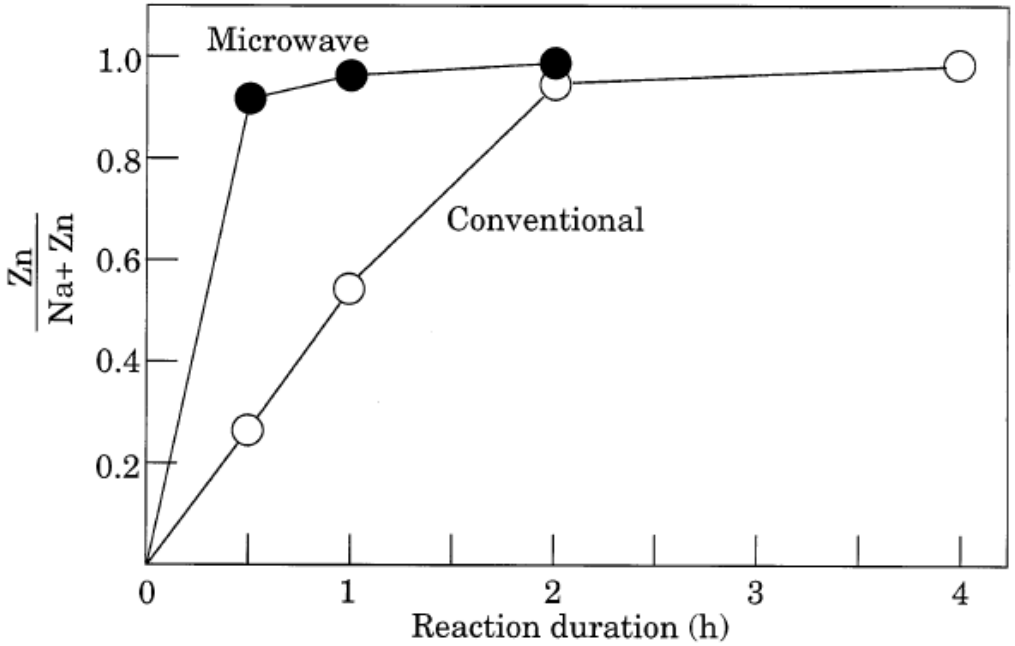

Hydrothermal Synthesis of $ZnBi_2O_6$

N. Kumada et al., Materials Research Bulletin, 33 (1998) 1411–1414.

Sonochemical / hydrothermal synthesis

Cavitation – the formation, growth, and implosion of bubbles
Generation of high amount of energy (formation of radicals)

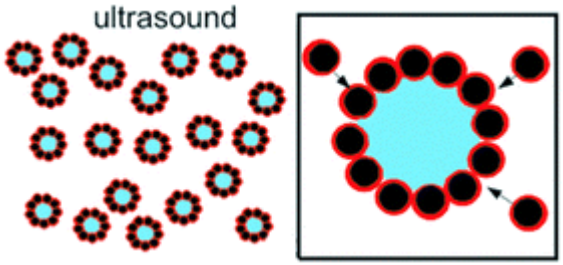

D. G. Shchukin, H. Möhwald, Phys. Chem. Chem. Phys. 8 (2006) 3496 – 3506.

Combined with hydrothermal synthesis

- Acceleration of crystallization
- Increase in the content of thermodynamically stable phases
- Initiation of redox reactions

In-situ methods to understand crystallization

P. Norby, Current Opinion in Colloid & Interface Science 11 (2006) 118–125.

Neutron diffraction

low intensity of neutron sources limits time resolution

Large samples – real autoclaves (Ti-Zr alloy)

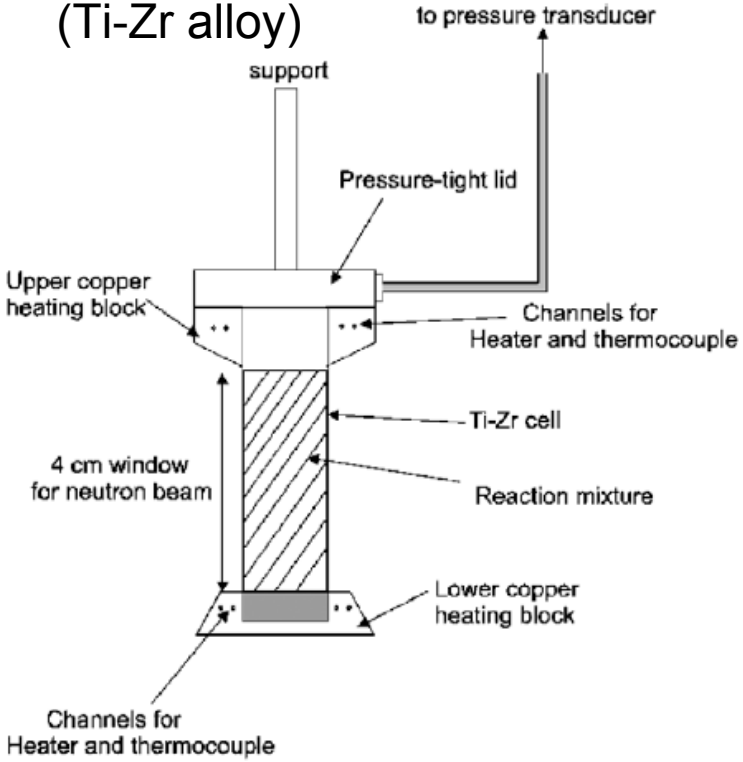

Fig. 1. A schematic of the reaction cell used for in-situ neutron diffraction studies of hydrothermal synthesis. The reaction cell is made from a null-scattering alloy, in order to eliminate scattering contribution from the reaction vessel. (With permission from Ref. [12].)

Synchrotron X-ray radiation

High intensity

Good time resolution (ms)

EDXRD: Big autoclaves

Angular dispersive XRD: Quartz tubes

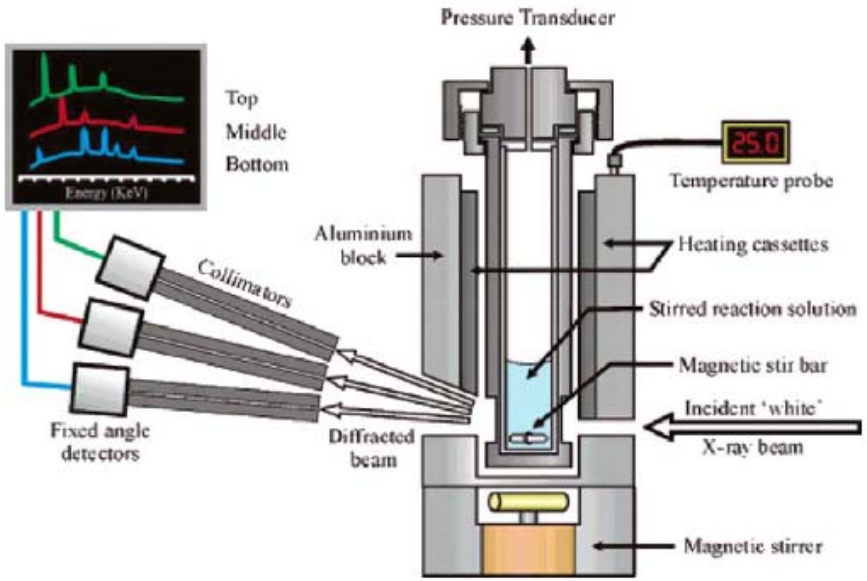

A schematic of the cell used for in-situ energy dispersive synchrotron X-ray powder diffraction studies at the SRS, Daresbury Laboratory. A three-element detector system is used for efficient detection of the EDXRD patterns.

In-situ methods to understand crystallization

P. Norby, Current Opinion in Colloid & Interface Science 11 (2006) 118–125.

ULM-n oxyfluorinated phosphates

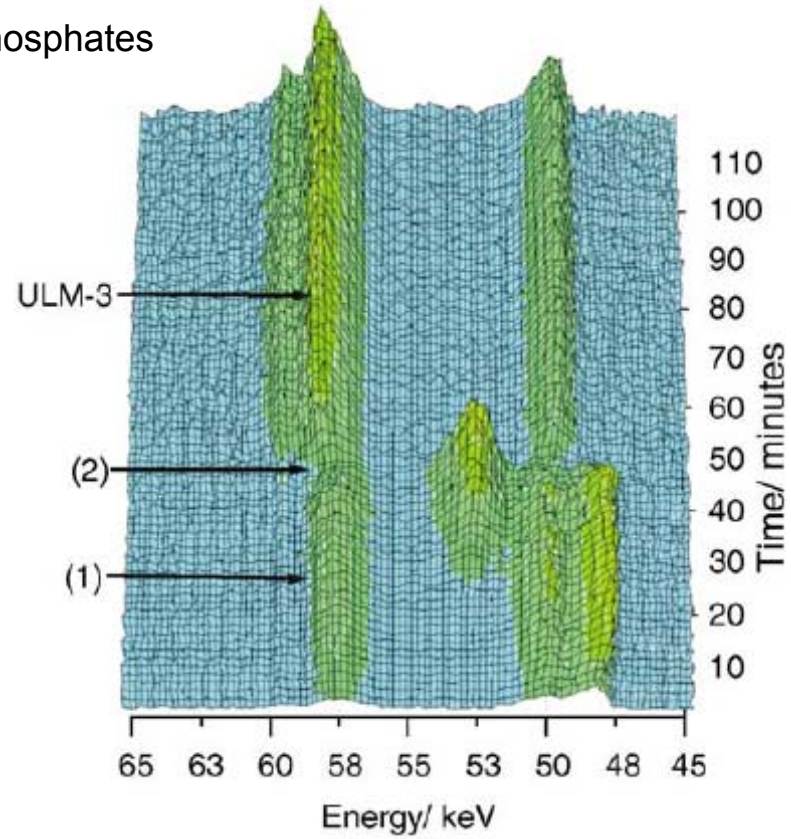

Fig. 6. A three-dimensional representation of part of the in-situ energy dispersive powder diffraction data collected during hydrothermal crystallization of ULM-3, showing the transient species. (With permission from Ref. [20].)

Investigation of mesoscopic structures

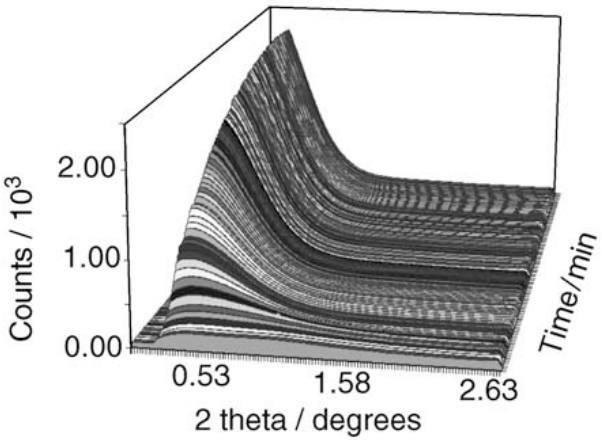

SAXS

$$n\lambda = 2d\,\sin(\theta)$$

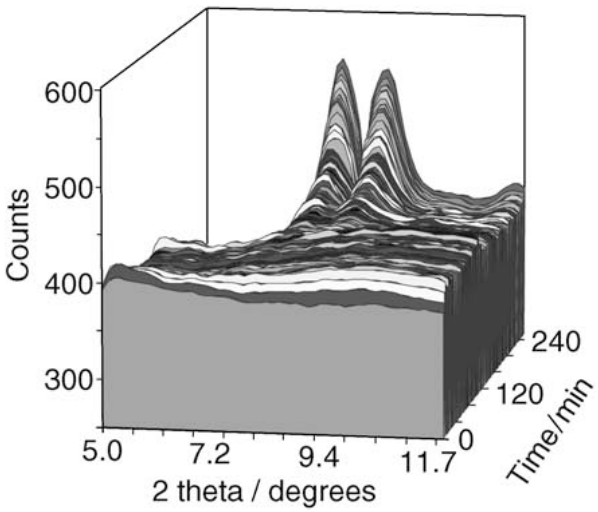

WAXS

Particle size distribution
Particle shape
Particle interaction

Crystallinity

G.A. Tompsett et al., ChemPhysChem 7 (2006) 296 – 319

Raman spectroscopy
FTIR spectroscopy in non-aqueous medium
UV-vis spectroscopy

Summary

Application of hydrothermal synthesis in catalyst preparation

- Stabilization of metastable phases
- Growth of single crystals
- Synthesis of inorganic materials with high-(phase-)purity
- Synthesis of nanostructuted catalysts

Parameters

- By varying the synthesis conditions (T,p,c, ...) it is possible to vary the particle size and change the morphology
    - Increase in time and concentration increases the particle size
    - Decrease of particle size to a certain critical size causes preferred formation of the phases with higher symmetry of the crystal lattice
- In complex systems predictions are difficult
- In situ studies of synthesis help to approach better understanding

Acknowledgements

Thank you for your attention!

Thanks to Almudena Celaya Sanfiz, Yury Kolenko, Wei Zhang, Gisela Weinberg, Zirong Tang, Frank Girgsdies and Edith Kitzelmann for synthesis, SEM and XRD of the examples